results indicate that temozolomide was especially beneficial to patients with tumors containing a highly methylated *MGMT* promoter. Methylation of the *MGMT* promoter is a strong predictor of response, overall survival, and time to disease progression in glioblastoma patients treated with temozolomide [13]. Both the *MGMT* methylation frequency and the proportion of highly methylated tumors are significantly higher for PCNSL than for glioblastoma (our unpublished data), which may explain why PCNSL patients responded to temozolomide. An analysis of more PCNSL patients is needed to evaluate the predictive power of *MGMT* methylation on the impact of salvage temozolomide treatment in PCNSL. Adjuvant therapy with temozolomide is also promising, and a phase III study on the use of HD-MTX and whole brain radiotherapy, with or without concomitant and adjuvant temozolomide, in PCNSL patients is being planned by the Japan Clinical Oncology Group Brain Tumor Study Group.

Acknowledgments This work was supported by a Grant-in-Aid for Scientific Research (C) from the Japan Society for the Promotion of Science (JSPS), 2008–2010. We thank Ms. Kyoko Totake and Mr. Makoto Yamashiro for their technical assistance.

References

1. Herrlinger U, Schabet M, Brugger W, Kortmann RD, Küker W, Deckert M, Engel C, Schmeck-Lindenau HJ, Mergenthaler HG, Krauseneck P, Benöhr C, Meisner C, Wiestler OD, Dichgans J, Kanz L, Bamberg M, Weller M (2002) German Cancer Society Neuro-Oncology Working Group NOA-03 multicenter trial of single-agent high-dose methotrexate for primary central nervous system lymphoma. Ann Neurol 51:247–252
2. Glass J, Gruber ML, Cher L, Hochberg FH (1994) Preirradiation methotrexate chemotherapy of primary central nervous system lymphoma: long-term outcome. J Neurosurg 81:188–195
3. O'Brien P, Roos D, Pratt G, Liew K, Barton M, Poulsen M, Olver I, Trotter G (2000) Phase II multicenter study of brief single-agent methotrexate followed by irradiation in primary CNS lymphoma. J Clin Oncol 18:519–526
4. Treon SP, Chabner BA (1996) Concepts in use of high-dose methotrexate therapy. Clin Chem 42:1322–1329
5. Hoang-Xuan K, Taillandier L, Chinot O, Soubeyran P, Bogdhan U, Hildebrand J, Frenay M, De Beule N, Delattre JY, Baron B, European Organization for Research, Treatment of Cancer Brain Tumor Group (2003) Chemotherapy alone as initial treatment for primary CNS lymphoma in patients older than 60 years: a multicenter phase II study (26952) of the European Organization for Research and Treatment of Cancer Brain Tumor Group. J Clin Oncol 21:2726–2731
6. O'Neill BP, O'Fallon JR, Earle JD, Colgan JP, Brown LD, Krigel RL (1995) Primary central nervous system non-Hodgkin's lymphoma: survival advantages with combined initial therapy? Int J Radiat Oncol Biol Phys 33:663–673
7. Schultz C, Scott C, Sherman W, Donahue B, Fields J, Murray K, Fisher B, Abrams R, Meis-Kindblom J (1996) Preirradiation chemotherapy with cyclophosphamide, doxorubicin, vincristine, and dexamethasone for primary CNS lymphomas: initial report of radiation therapy oncology group protocol 88-06. J Clin Oncol 14:556–564
8. Newlands ES, Stevens MF, Wedge SR, Wheelhouse RT, Brock C (1997) Temozolomide: a review of its discovery, chemical properties, pre-clinical development and clinical trials. Cancer Treat Rev 23:35–61
9. Herrlinger U, Küker W, Platten M, Dichgans J, Weller M (2002) First-line therapy with temozolomide induces regression of primary CNS lymphoma. Neurology 58:1573–1574
10. Lerro KA, Lacy J (2002) Case report: a patient with primary CNS lymphoma treated with temozolomide to complete response. J Neurooncol 59:165–168
11. Omuro AM, Taillandier L, Chinot O, Carnin C, Barrie M, Hoang-Xuan K (2007) Temozolomide and methotrexate for primary central nervous system lymphoma in the elderly. J Neurooncol 85:207–211
12. Reni M, Zaja F, Mason W, Perry J, Mazza E, Spina M, Bordonaro R, Ilariucci F, Faedi M, Corazzelli G, Manno P, Franceschi E, Pace A, Candela M, Abbadessa A, Stelitano C, Latte G, Ferreri AJ (2007) Temozolomide as salvage treatment in primary brain lymphomas. Br J Cancer 96:864–867
13. Hegi ME, Diserens AC, Gorlia T, Hamou MF, de Tribolet N, Weller M, Kros JM, Hainfellner JA, Mason W, Mariani L, Bromberg JE, Hau P, Mirimanoff RO, Cairncross JG, Janzer RC, Stupp R (2005) MGMT gene silencing and benefit from temozolomide in glioblastoma. N Engl J Med 352:997–1003
14. Everhard S, Kaloshi G, Crinière E, Benouaich-Amiel A, Lejeune J, Marie Y, Sanson M, Kujas M, Mokhtari K, Hoang-Xuan K, Delattre JY, Thillet J (2006) MGMT methylation: a marker of response to temozolomide in low-grade gliomas. Ann Neurol 60:740–743
15. Esteller M, Gaidano G, Goodman SN, Zagonel V, Capello D, Botto B, Rossi D, Gloghini A, Vitolo U, Carbone A, Baylin SB, Herman JG (2002) Hypermethylation of the DNA repair gene O(6)-methylguanine DNA methyltransferase and survival of patients with diffuse large B-cell lymphoma. J Natl Cancer Inst 94:26–32
16. Margison GP, Santibanez-Koref MF (2002) O^6-alkylguanine-DNA alkyltransferase: role in carcinogenesis and chemotherapy. Bioessays 24:255–256
17. Gerson SL (2004) MGMT: its role in cancer aetiology and cancer therapeutics. Nat Rev Cancer 4:296–307
18. Karran P, Bignami M (1994) DNA damage tolerance, mismatch repair and genome instability. Bioessays 16:833–839
19. Gerson SL (2002) Clinical relevance of MGMT in the treatment of cancer. J Clin Oncol 20:2388–2399
20. Becker K, Gregel CM, Kaina B (1997) The DNA repair protein O^6-methylguanine-DNA methyltransferase protects against skin tumor formation induced by antineoplastic chloroethylnitrosourea. Cancer Res 57:3335–3338
21. Sakumi K, Shiraishi A, Shimizu S, Tsuzuki T, Ishikawa T, Sekiguchi M (1997) Methylnitrosourea-induced tumorigenesis in MGMT gene knockout mice. Cancer Res 57:2415–2418
22. Danam RP, Qian Howell SR, Brent TP (1999) Methylation of selected CpGs in the human O^6-methylguanine-DNA methyltransferase promoter region as a marker of gene silencing. Mol Carcinog 24(2):85–89
23. Esteller M, Hamilton SR, Burger PC, Baylin SB, Herman JG (1999) Inactivation of the DNA repair gene O^6-methylguanine-DNA methyltransferase by promoter hypermethylation is a common event in primary human neoplasia. Cancer Res 59:793–797
24. Wojdacz TK, Hansen LL (2006) Reversal of PCR bias for improved sensitivity of the DNA methylation melting curve assay. Biotechniques 41:274–278

25. Wojdacz TK, Dobrovic A (2007) Methylation-sensitive high resolution melting (MS-HRM): a new approach for sensitive and high-throughput assessment of methylation. Nucleic Acids Res 35:e41
26. Ogino S, Kawasaki T, Brahmandam M, Cantor M, Kirkner GJ, Spiegelman D, Makrigiorgos GM, Weisenberger DJ, Laird PW, Loda M, Fuchs CS (2006) Precision and performance characteristics of bisulfite conversion and real-time PCR (MethyLight) for quantitative DNA methylation analysis. J Mol Diagn 8:209–217
27. Palmisano WA, Divine KK, Saccomanno G, Gilliland FD, Baylin SB, Herman JG, Belinsky SA (2000) Predicting lung cancer by detecting aberrant promoter methylation in sputum. Cancer Res 60:5954–5958
28. Pike BL, Greiner TC, Wang X, Weisenburger DD, Hsu YH, Renaud G, Wolfsberg TG, Kim M, Weisenberger DJ, Siegmund KD, Ye W, Groshen S, Mehrian-Shai R, Delabie J, Chan WC, Laird PW, Hacia JG (2008) DNA methylation profiles in diffuse large B-cell lymphoma and their relationship to gene expression status. Leukemia 22:1035–1043
29. Uccella S, Cerutti R, Placidi C, Marchet S, Carnevali I, Bernasconi B, Proserpio I, Pinotti G, Tibiletti MG, Furlan D, Capella C (2009) MGMT methylation in diffuse large B-cell lymphoma: validation of quantitative methylation-specific PCR and comparison with MGMT protein expression. J Clin Pathol 62:715–723
30. Kurzwelly D, Glas M, Roth P, Weimann E, Lohner H, Waha A, Schabet M, Reifenberger G, Weller M, Herrlinger U (2009) Primary CNS lymphoma in the elderly: temozolomide therapy and MGMT status. J Neurooncol 97:389–392
31. Vlassenbroeck I, Califice S, Diserens AC, Migliavacca E, Straub J, Di Stefano I, Moreau F, Hamou MF, Renard I, Delorenzi M, Flamion B, DiGuiseppi J, Bierau K, Hegi ME (2008) Validation of real-time methylation-specific PCR to determine O^6-methylguanine-DNA methyltransferase gene promoter methylation in glioma. J Mol Diagn 10:332–337

Phosphorylation of dedicator of cytokinesis 1 (Dock180) at tyrosine residue Y722 by Src family kinases mediates EGFRvIII-driven glioblastoma tumorigenesis

Haizhong Feng[a,b], Bo Hu[a,c,1], Michael J. Jarzynka[a,b,2], Yanxin Li[d], Susan Keezer[e], Terrance G. Johns[f], Careen K. Tang[g], Ronald L. Hamilton[b], Kristiina Vuori[h], Ryo Nishikawa[i], Jann N. Sarkaria[j], Tim Fenton[k,3], Tao Cheng[d,l], Frank B. Furnari[k], Webster K. Cavenee[k,1], and Shi-Yuan Cheng[a,b,1]

[a]University of Pittsburgh Cancer Institute, Departments of [b]Pathology, [c]Medicine, and [d]Radiation Oncology, University of Pittsburgh School of Medicine, Pittsburgh, PA 15213; [e]Cell Signaling Technology, Inc., Danvers, MA 01923; [f]Oncogenic Signaling Laboratory, Monash Institute of Medical Research, Clayton, Victoria 3168, Australia; [g]Department of Oncology, Lombardi Comprehensive Cancer Center, Georgetown University Medical Center, Washington, DC 20057; [h]Cancer Center, Sanford-Burnham Medical Research Institute, La Jolla, CA 92037; [i]Department of Neurosurgery, Saitama Medical University, Saitama 350-0495, Japan; [j]Department of Radiation Oncology, Mayo Clinic, Rochester, MN 55905; [k]Ludwig Institute for Cancer Research, University of California at San Diego School of Medicine, La Jolla, CA 92093; and [l]State Key Laboratory of Experimental Hematology, Institute of Hematology and Blood Diseases Hospital, Center for Stem Cell Medicine, Chinese Academy of Medical Sciences and Peking Union Medical College, Tianjin 300041, China

Contributed by Webster K. Cavenee, December 29, 2011 (sent for review November 30, 2011)

Glioblastoma, the most common primary malignant cancer of the brain, is characterized by rapid tumor growth and infiltration of tumor cells throughout the brain. These traits cause glioblastomas to be highly resistant to current therapies with a resultant poor prognosis. Although aberrant oncogenic signaling driven by signature genetic alterations, such as EGF receptor (EGFR) gene amplification and mutation, plays a major role in glioblastoma pathogenesis, the responsible downstream mechanisms remain less clear. Here, we report that EGFRvIII (also known as ΔEGFR and de2-7EGFR), a constitutively active EGFR mutant that is frequently co-overexpressed with EGFR in human glioblastoma, promotes tumorigenesis through Src family kinase (SFK)-dependent phosphorylation of Dock180, a guanine nucleotide exchange factor for Rac1. EGFRvIII induces phosphorylation of Dock180 at tyrosine residue 722 (Dock180^{Y722}) and stimulates Rac1-signaling, glioblastoma cell survival and migration. Consistent with this being causal, siRNA knockdown of Dock180 or expression of a Dock180^{Y722F} mutant inhibits each of these EGFRvIII-stimulated activities. The SFKs, Src, Fyn, and Lyn, induce phosphorylation of Dock180^{Y722} and inhibition of these SFKs by pharmacological inhibitors or shRNA depletion markedly attenuates EGFRvIII-induced phosphorylation of Dock180^{Y722}, Rac1 activity, and glioblastoma cell migration. Finally, phosphorylated Dock180^{Y722} is coexpressed with EGFRvIII and phosphorylated Src^{Y418} in clinical specimens, and such coexpression correlates with an extremely poor survival in glioblastoma patients. These results suggest that targeting the SFK-p-Dock180^{Y722}-Rac1 signaling pathway may offer a novel therapeutic strategy for glioblastomas with EGFRvIII overexpression.

invasion | Akt

Oncogenic signaling stimulated by overexpressed genes, such as EGF receptor (EGFR), renders human brain glioblastomas malignant and resistant to combination therapies (1). Amplification of EGFR is the most frequent genetic alteration in World Health Organization (WHO) grade IV glioblastoma multiforme (GBM) (2, 3) and is associated with poor prognosis (1). About half of GBMs with EGFR amplification also express the mutant form, EGFRvIII/ΔEGFR/de2-7EGFR, that lacks a portion of the extracellular ligand-binding domain (encoded by exons 2 through 7), leading to constitutively activated oncogenic signaling (3, 4). Expression of EGFRvIII enhances glioblastoma tumorigenicity in vivo (5) and promotes glioblastoma cell motility in vitro (6). Although EGFRvIII activates PI3K/Akt signaling, other signaling cascades are also likely involved in mediating EGFRvIII-driven tumorigenesis (3, 4).

Dedicator of cytokinesis 1 (Dock1 or Dock180) is a guanine nucleotide exchange factor (GEF) that activates Rac1 and controls several cellular functions, including cell motility, survival, and proliferation (7). Dock180 facilitates nucleotide exchange on Rac1 through its Dock-homology region-2 (DHR-2) domain, but requires binding to engulfment and cell motility protein 1 (ELMO1) through its N-terminal SH3 domain to achieve full activation of Rac1 (8). Adjacent to the SH3 region resides a DHR-1 domain which interacts with phosphatidyl-inositol(3,4,5)P_3 (PIP_3), and thereby mediates the localization of Dock180 to the cell membrane sites of PIP_3 production where Dock180 subsequently activates Rac1 through its DHR-2 domain (8). Although genomic studies have revealed no genetic alterations in Rac1, Dock180, or ELMO1 in various human cancers, including glioblastoma, it remains possible, given its central role in regulating cellular functions, that GEF-Rac1 signaling is stimulated by signals emanating from activated oncogenes, such as EGFRvIII.

GEF activation by receptor tyrosine kinases (RTK) stimulates Rac1 (9) and may be important in EGFRvIII-driven tumorigenesis (3). Dock180 activates Rac1 (8) and is involved in RTK-induced cell migration in *Drosophila* (10), and Dock180 plays a role in glioblastoma cell invasion through the activation of Rac1 (11). Here, we report that EGFRvIII induces tyrosine phosphorylation (p-Y) at tyrosine residue 722 (Y722) of Dock180, and that Dock180 and its phosphorylation are required for EGFRvIII-promoted glioblastoma cell growth, survival, and invasion. Correspondingly, ectopic expression of an unphosphorylatable Dock180^{Y722F} mutant inhibited EGFRvIII-induced Rac1 activation, cell migration, and survival in vitro, and glioblastoma growth and invasion in the brain. We also report that EGFRvIII-induced p-Dock180^{Y722} is dependent on Src family kinases (SFKs), that p-Dock180^{Y722} is coexpressed with EGFRvIII and pan-p-Src^{Y418} in clinical glioblastoma specimens, and that such coexpression correlates with an extremely poor prognosis.

Results

Dock180 Is Required for EGFRvIII-Promoted Glioblastoma Cell Migration and Survival in Vitro. To determine if EGFRvIII signaling engages Dock180 as part of its oncogenic mechanism, we

Author contributions: H.F., B.H., and S.-Y.C. designed research; H.F., B.H., M.J.J., and Y.L. performed research; S.K., T.G.J., C.K.T., R.L.H., K.V., R.N., J.N.S., T.F., T.C., F.B.F., and W.K.C. contributed new reagents/analytic tools; H.F., B.H., and S.-Y.C. analyzed data; and H.F., B.H., F.B.F., W.K.C., and S.-Y.C. wrote the paper.

The authors declare no conflict of interest.

[1]To whom correspondence may be addressed. E-mail: hub@upmc.edu, wcavenee@ucsd.edu, or chengs@upmc.edu.

[2]Present Address: Department of Pharmacy, University of Pittsburgh Medical Center-Chartwell, Pittsburgh, PA 15205.

[3]Present Address: Laboratory of Viral Oncology, University College London Cancer Institute, London WC1E 6BT, England.

This article contains supporting information online at www.pnas.org/lookup/suppl/doi:10.1073/pnas.1121457109/-/DCSupplemental.

stably expressed exogenous EGFRvIII in glioblastoma LN444/GFP and SNB19/GFP cells that have high levels of endogenous Dock180 (11). Expression of EGFRvIII in LN444 and SNB19 glioblastoma cells induced p-EGFRvIII, p-Akt, p-Erk1/2, and Rac1 activity (Fig. 1*A*), increased in vitro cell migration (Fig. 1*B*), proliferation (Fig. S1 *A* and *B*), and markedly inhibited cell apoptosis (Fig. S1*C*).

We recently reported that Dock180 promotes glioblastoma cell invasion through activation of Rac1 (11). To determine whether this function of Dock180 is required for EGFRvIII-stimulated glioblastoma tumorigenesis, we knocked down endogenous Dock180 using siRNAs (11) in each of LN444/GFP, LN444/GFP/EGFRvIII, SNB19/GFP, and SNB19/GFP/EGFRvIII cells. As shown in Fig. 1*C*, knockdown of Dock180 in EGFRvIII-expressing cells inhibited EGFRvIII-induced p-Akt, p-Erk1/2, and Rac1 activity. Depletion of Dock180 also suppressed basal Rac1 activity in GFP control cells (11). Knockdown of Dock180 attenuated EGFRvIII-promoted cell migration and survival in EGFRvIII-expressing cells and basal levels of cell migration in GFP control cells (Fig. 1 *D* and *E*). However, depletion of Dock180 had only moderate effects on cell proliferation in both EGFRvIII- and GFP-expressing cells (Fig. 1 *F* and *G*). These data suggest that Dock180 is critical for EGFRvIII-stimulated p-Akt, p-Erk1/2, and Rac1 activity, as well as for glioblastoma cell migration and survival in vitro.

EGFRvIII Induces p-Y of Dock180 at Y722. We examined whether EGFRvIII phosphorylates Dock180 at Y residues in glioblastoma cells. As shown in Fig. 2*A*, p-Y of endogenous Dock180 was evident in both LN444/EGFRvIII and SNB19/EGFRvIII cells, but not in GFP-expressing cells. To identify the Y residues of Dock180 that are phosphorylated by EGFRvIII, we generated Flag-tagged WT and six different Dock180 mutants that lack DHR-1, -2, or other regions (Fig. 2*B*). When EGFRvIII and WT Dock180 were coexpressed in HEK293T cells, EGFRvIII induced p-Y of WT Dock180, whereas expression of either protein alone did not result in p-Y of Dock180 (Fig. 2*C*). Next, we coexpressed EGFRvIII with WT or the six individual mutants of Dock180 and found a marked reduction of EGFRvIII-induced p-Y of the Dock180 Del-6 mutant but not the Dock180 WT or other Del mutants (Fig. 2*D*, blue arrows), suggesting that the p-Y sites are located between amino acid residues 602 and 805 (Fig. 2*B*). In this region, there are six Y residues: Y700, Y712, Y722, Y736, Y760, and Y780. To identify which Y residue is phosphorylated by EGFRvIII, we individually mutated each of these six Y residues to a phenylalanine (F) in the Dock180 Del-5 mutant. When these six Del-5 YF mutants or the Del-5 mutant were separately coexpressed with EGFRvIII in HEK293T cells, EGFRvIII induced p-Y of all Dock180 mutants except Del-5/F722, suggestive of Y722 as a potential p-Y site by EGFRvIII (Fig. 2*E*). To further validate this finding, we generated an Y722F mutation in the full-length Dock180 protein (Dock180^{Y722F}). Coexpression of EGFRvIII with Dock180^{Y722F} showed a more than 40% reduction in p-Y levels compared with that of Dock180^{WT} (Fig. 2*F*). These data suggest that Y722 is a major p-Y site induced by EGFRvIII, and that there are additional p-Y sites within Dock180 because of EGFRvIII activity to a lesser extent. Next, we compared amino acid sequences surrounding Y722 in Dock180 in various species and the other four members of the Dock family, and found that Y722 and most of its surrounding residues are highly conserved among them (Fig. 2*G*).

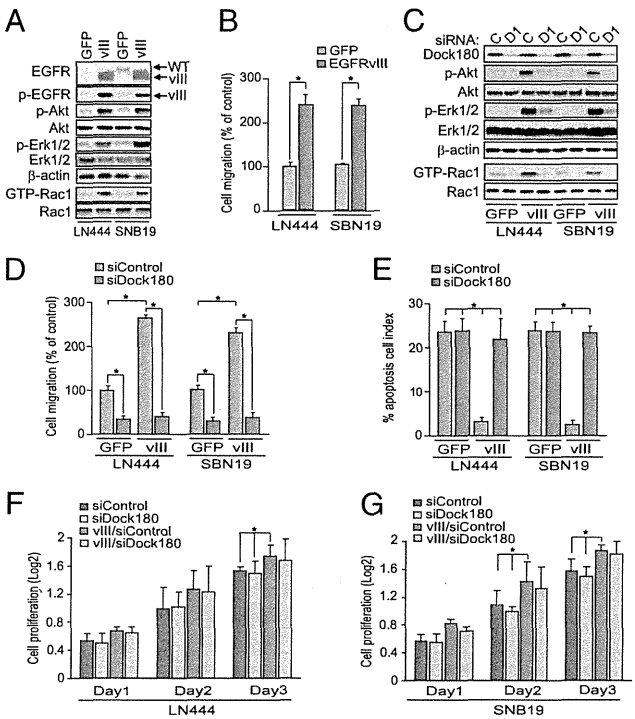

Fig. 1. Dock180 is required for EGFRvIII-induced Rac1 activity, glioblastoma cell migration, and survival in vitro. (*A*) IB analyses. (*B* and *D*) In vitro cell migration assays. Data are presented as percentage of control cells. (*C*) IB analyses. C, control siRNA; D1, Dock180 siRNA pool. In *A* and C, β-actin, Akt, Erk1/2, and Rac1 were used as loading controls. (*E*) Cell apoptosis. Data are presented as percentage of apoptotic cells. (*F* and *G*) Cell proliferation; data were calculated by dividing the total cell number by 50,000 and converting it to a $\log_2$ value. Data in *B* and *D*–*G* were from six replicates per pair per cell line. Data are representative from three independent experiments with similar results. $^*P < 0.05$. (Scale bars, ± SD.)

Phosphorylation of Dock180^{Y722} Is Required for EGFRvIII-Promoted Glioblastoma Tumorigenesis. We generated a rabbit polyclonal antibody that specifically recognizes the p-Dock180^{Y722} protein. This anti–p-Dock180^{Y722} antibody detected EGF (but not PDGF or HGF) induced p-Y of endogenous Dock180 in SNB19, U87, U373, and LN444 glioblastoma cells at various levels (Fig. 3*A*). We then knocked down Dock180 in SNB19 or SNB19/EGFRvIII cells using an siRNA pool for Dock180 or a control siRNA (11), and found that depletion of endogenous Dock180 by the siRNA pool, but not control siRNA, significantly diminished the EGFRvIII-induced p-Dock180^{Y722} in SNB19/EGFRvIII cells whereas no signal was seen in SNB19 cells (Fig S2 *A* and *B*). These results validate the specificity of this antibody in detecting EGFRvIII-induced p-Y722 of endogenous Dock180 in glioblastoma cells. Next, we stably transfected Flag-tagged Dock180^{WT} or Dock180^{Y722F} into EGFRvIII-expressing SNB19 and LN444 glioblastoma cells. As shown in Fig. 3*B*, ectopic expression of Dock180^{WT} did not affect EGFRvIII stimulation of p-Akt, p-Erk1/2, and Rac1 activity in SNB19/EGFRvIII and LN444/EGFRvIII cells. In contrast, expression of Dock180^{Y722F} markedly reduced EGFRvIII-induced p-Akt, p-Erk1/2, and Rac1 activity. Additionally, Dock180^{Y722F} but not Dock180^{WT} significantly attenuated EGFRvIII-stimulated glioblastoma cell survival and migration in vitro (Fig. S3 *A* and *B*). However, expression of Dock180^{WT} or Dock180^{Y722F} had only a moderate impact on in vitro proliferation in both LN444/EGFRvIII and SNB19/EGFRvIII cells (Fig. S3 *C* and *D*).

We then separately implanted SNB19/EGFRvIII/Dock180^{WT}, SNB19/EGFRvIII/Dock180^{Y722F}, or the control SNB19/EGFRvIII/GFP cells into the brains of mice. As described previously (12), SNB19/GFP cells formed small but invasive tumors in the brains of mice. Moreover, mice that received SNB19/EGFRvIII/GFP cells showed markedly enhanced tumor growth and invasion, whereas mice that received SNB19/EGFRvIII/Dock180^{WT} cells also developed brain tumors with large volumes and similar invasiveness (Fig. 3*C* and Fig. S4 *A*–*C*), suggesting no further enhancement by Dock180^{WT} expression. In contrast, mice that received SNB19/EGFRvIII/Dock180^{Y722F} cells developed much smaller and less invasive tumors (Fig. 3*C* and Fig. S4 *A*–*C*). In addition, expression of Dock180^{WT} had no significant effect on glioblastoma cell proliferation and survival compared with the controls (Fig. 3 *D* and *E*,

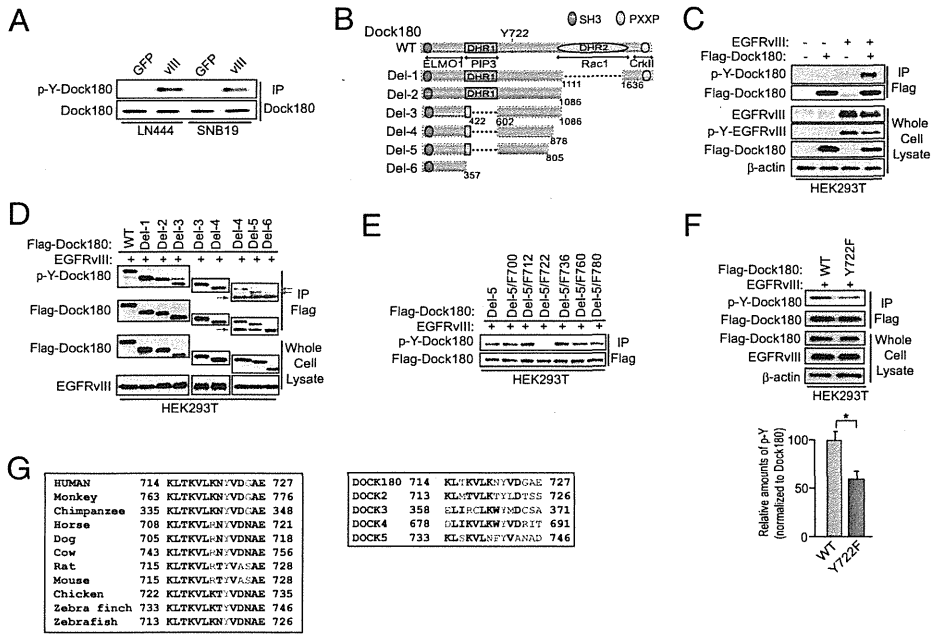

Fig. 2. EGFRvIII induces p-Y of Dock180 at Y722. (*A*) IP and IB analyses. (*B*) Schematic of deletion mutants of Dock180. (*C*) EGFRvIII induces p-Y of Dock180 in HEK293T cells. (*D*) IB analyses. Red arrows, IgG; blue arrows, p-Y of Del mutant. (*E*) Mutation of Y722F in Del-5 decreased p-Y of Dock180. (*F*) Y722 is a major EGFRvIII-induced p-Y site in Dock180. (Scale bars, ± SD.) Bar graph underneath: relative amount of p-Y of Dock180 was determined from three separate in IP-IB blots by ImageJ and normalized to the amount of Dock180. $*P < 0.05$. (*G*) Y722 is conserved in Dock180 of various species and in Dock protein family. Black, conserved amino acids; blue, nonconserved amino acids. In *A* and *C–F*, a pan-phospho-tyrosine antibody was used to detect p-Y-Dock180. Data are representative of three independent experiments with similar results.

and Fig. S4*A*). However, expression of Dock180^{Y722F} significantly suppressed EGFRvIII-stimulated glioblastoma cell proliferation and survival compared with SNB19/EGFRvIII/GFP or SNB19/EGFRvIII/Dock180^{WT} tumors (Fig. 3 *D* and *E* and Fig. S4*A*). These data suggest that p-Dock180^{Y722} is important for EGFRvIII-promoted glioblastoma tumorigenesis in vivo and that Dock180^{Y722F} acts in a dominant negative fashion to inhibit EGFRvIII-driven tumorigenicity.

SFKs Are Responsible for EGFRvIII-Induced p-Dock180^{Y722}. We next performed in silico analyses (http://scansite.mit.edu) and found that Y722 of Dock180 is a potential p-Y site for Src. To determine whether Src and other SFKs are involved in EGFRvIII-stimulated p-Dock180^{Y722} and cell migration, we first treated LN444/EGFRvIII and SNB19/EGFRvIII cells with two pharmacological inhibitors of SFKs (SU6656, PP2) or a vehicle control. As shown in Fig. 4 *A* and *B*, both PP2 and SU6656 effectively inhibited EGFRvIII-induced p-Y of Dock180, Rac1 activity, pan p-Y of Src^{Y418}, and EGFRvIII-stimulated cell migration.

Next, we coexpressed WT, kinase dead (KD) or constitutively activated (CA) Src with flag-tagged Dock180^{WT} or Dock180^{Y722F} in HEK293T cells. WT or CA Src induced p-Y of Dock180^{WT} to higher levels compared with that of Dock180^{Y722F}, whereas KD Src had no effect on p-Y of Dock180^{WT} or Dock180^{Y722F}. As expected, CA Src displayed higher kinase activity on p-Y of Dock180 than did WT Src (Fig. 4*C*). We then tested whether the dominant negative KD Src mutant inhibits the EGFRvIII-induced p-Y of Dock180. As shown in Fig. 4*D*, coexpression of KD

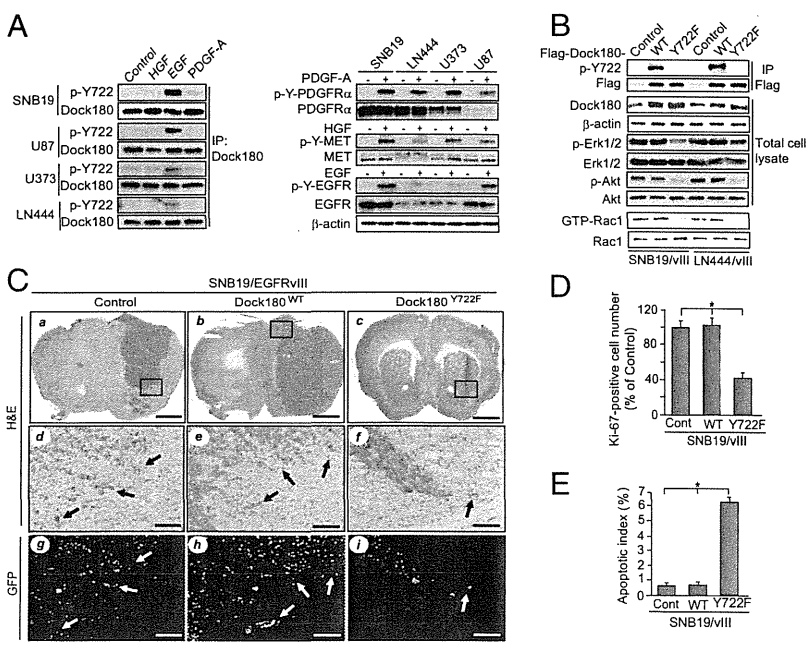

Fig. 3. Phosphorylation of Dock180^{Y722} is critical for EGFRvIII-driven glioblastoma growth and invasion. (*A*) EGF, but not PDGF-A or HGF, induces p-Y of endogenous Dock180^{Y722} (detected with a specific anti–p-Dock180^{Y722} antibody) in glioblastoma cells. (*B*) Effect of Dock180^{WT}, Dock180^{Y722F}, or a vector control on p-Dock180^{Y722}, p-Akt, p-Erk1/2, and Rac1 activity in EGFRvIII-expressing cells. Dock180, Akt, Erk1/2, Rac1, and β-actin were used as loading controls. (*C*) Dock180^{Y722F} inhibits EGFRvIII-promoted glioblastoma growth and invasion in the brain. Representative H&E and IHC images of brain sections of mice receiving various SNB19 cells (8 wk postinjection, five mice per group). (*a–c*) H&E staining. (Scale bars, 1 mm.) (*d–f*) Enlarged areas in a to c marked with squares. (Scale bars, 200 μm.) (*g–i*) GFP images of the same areas in *d* to *f*. (Scale bars, 200 μm.) Arrows indicate invasive tumor cells (*d–i*). (*D* and *E*) Quantification of Ki-67 and TUNEL staining, respectively. $*P < 0.05$. (Scale bars, ± SD.) Data represent three independent experiments with similar results.

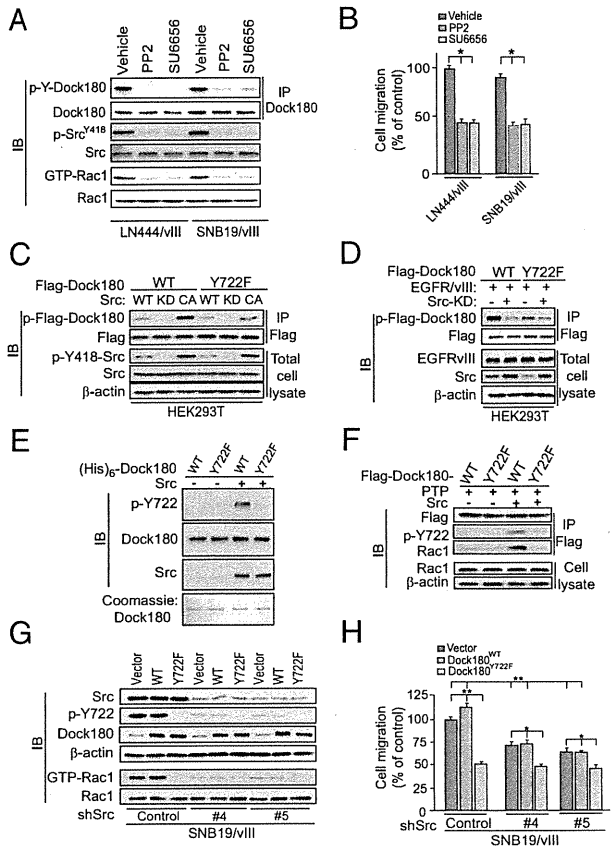

Fig. 4. EGFRvIII-induced p-Dock180^{Y722} is Src-dependent. (*A*) Inhibition of Src by PP2 (2 μM) or SU6656 (2 μM) attenuates EGFRvIII-stimulated p-Y of Dock180 (detected with a pan-phospho-tyrosine antibody, 4G10) and Rac1 activity. (*B*) In vitro cell migration. (*C*) Src phosphorylates Dock180 at Y722 by Src. Dock180^{WT} or Dock180^{Y722F} and WT, a KD or a CA Src were separately coexpressed in HEK293T cells. (*D*) Src-KD inhibits EGFRvIII-induced p-Dock180^{Y722}. (*E*) In vitro Src kinase assay. Various proteins were visualized by Coomassie brilliant blue staining. (*F*) Src-dependent p-Y of Dock180 at Y722 enhances association of Dock180 with Rac1. (*G*) Knockdown of Src inhibits EGFRvIII-induced p-Dock180^{Y722} and Rac1 activation. (*H*) In vitro cell migration. In *A* and *C*–*G*, Dock180, Src, Rac1, and β-actin were used as loading controls. In *A*, *C*, and *D*, a pan anti–p-Y antibody (4G10) was used to detect p-Y of Dock180. (*E*–*G*) A specific anti–p-Dock180^{Y722} antibody was used to detect p-Y722 of Dock180. In *B* and *H*, data are presented as percentage of the control from six replicates per pair per cell line. *$P < 0.05$ and **, $P < 0.01$. (Scale bars, ± SD.) Data represent three independent experiments with similar results.

Src with EGFRvIII and Dock180 partially blocked EGFRvIII-induced p-Y of both Dock180^{WT} and Dock180^{Y722F} compared with controls. These results are consistent with partial attenuation of EGFRvIII-induced p-Y by the Dock180^{Y722F} mutant, suggesting that there are other p-Y sites on Dock180 stimulated by EGFRvIII through other kinases.

To validate direct Src phosphorylation of Dock180^{Y722}, we performed in vitro p-Y assays by incubating purified recombinant (His)$_6$-Dock180^{WT} or (His)$_6$-Dock180^{Y722F} proteins with a recombinant active Src followed by immunoblot (IB) using the specific anti–p-Dock180^{Y722} antibody. As shown in Fig. 4*E*, a recombinant Src effectively induced p-Y of Dock180^{WT} but not Dock180^{Y722F} in vitro. Next, we evaluated the impact of Src-induced p-Y of Dock180 on its interaction with Rac1 using an in vitro reconstitution assay. In the absence of the recombinant Src, when immunoprecipitated Dock180^{WT} or Dock180^{Y722F} from HEK293T was dephosphorylated by a protein tyrosine phosphatase, p-Y of Y722 of Dock180 was undetectable and minimal Dock180–Rac1 interaction was observed. However, when a recombinant Src was added, p-Dock180^{WT} but not p-Dock180^{Y722F} was significantly induced, accompanied with an increase in association of Dock180 with Rac1 (Fig. 4*F*).

Then, we stably knocked down endogenous Src using two different shRNAs in SNB19/EGFRvIII cells that expressed either Dock180^{WT} or Dock180^{Y722F}. An ~75% reduction of Src in SNB19/EGFRvIII cells markedly attenuated EGFRvIII-stimulated p-Y722 of Dock180, Rac1 activity (Fig. 4*G*) and cell migration (Fig. 4*H*) in vector control and Dock180^{WT}-expressing cells, but had a minimal impact on Dock180^{Y722F}-expressing cells. Additionally, expression of Dock180^{WT} had minimal impact, whereas Dock180^{Y722F} suppressed EGFRvIII stimulation of p-Dock180^{Y722}, Rac1 activity, and cell migration (Fig. 4 *G* and *H*).

Finally, we determined whether two other SFKs, Fyn and Lyn (13, 14), are involved in EGFRvIII-stimulated Dock180 phosphorylation. We knocked down endogenous Fyn or Lyn using two separate shRNAs for each protein in SNB19/EGFRvIII cells that express Dock180^{WT}, Dock180^{Y722F}, or a vector control. As shown in Fig. 5 *A*–*C*, shRNA knockdown of Fyn or Lyn markedly decreased EGFRvIII-induced p-Y722 of Dock180^{WT}, Rac1 activity, and cell migration in SNB19/EGFRvIII/vector and SNB19/EGFRvIII/Dock180^{WT} cells, but did not affect EGFRvIII stimulation of SNB19/EGFRvIII/Dock180^{Y722F} cells (Fig. 5). These data demonstrate that SFKs, Src, Fyn, and Lyn largely mediate EGFRvIII stimulation of Rac1 activity and glioblastoma cell migration through p-Y722 of Dock180.

SFKs Stimulate p-Dock180^{Y722}, Rac1 Activity, and Cell Migration of Primary Human GBM Cells That Overexpress EGFRvIII. Next, we determined whether SFKs also induce p-Y of Dock180^{Y722}, Rac1 activity, and cell migration in primary human GBM cells. To this end, we examined cells from four different serially transplanted human GBMs, GBM6, GBM39, GBM12, and GBM14 cells that retain the EGFR status of the primary tumor from which they were derived (15). In GBM6 and GBM39 that retained EGFRvIII overexpression, strong p-Y of Dock180^{Y722} and Rac1 activity were found (Fig. S5*A*). In contrast, without EGF stimulation, neither p-Y722 of Dock180 nor increased Rac1 activity was detected in GBM12 cells that express WT EGFR or GBM14 cells that have nondetectable WT EGFR or EGFRvIII. We then treated GBM6 and GBM39 cells with the EGFR inhibitors AG1478 and Erlotinib, the SFK inhibitors SU6656, PP2, its inactive stereoisomer PP3, or vehicle control. These inhibitors markedly attenuated EGFRvIII-induced pan-p-Src^{Y418}, p-Dock180^{Y722}, p-Akt, p-Erk1/2,

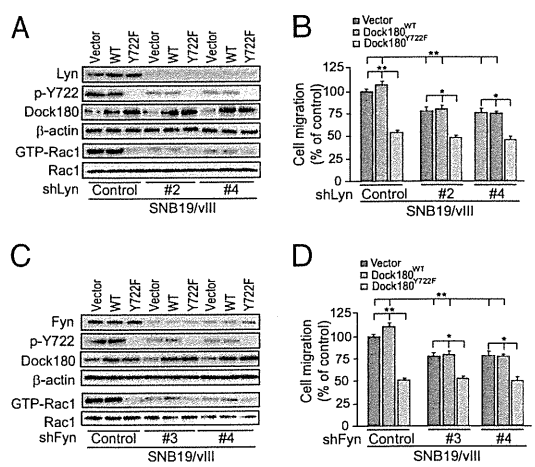

Fig. 5. EGFRvIII-induced p-Dock180^{Y722} is also dependent on SFKs, Fyn and Lyn. (*A* and *C*) Knockdown of Lyn or Fyn inhibits EGFRvIII-induced p-Dock180^{Y722} and Rac1 activation. Dock180, Rac1, and β-actin were used as loading controls. (*B* and *D*) In vitro cell migration assays; data are presented as percentage of the control from six replicates per pair per cell line. *$P < 0.05$ and **, $P < 0.01$. (Scale bars, ± SD.) Data represent three independent experiments with similar results.

Rac1 activity, and cell migration compared with GBM cells treated with PP3 or vehicle control (Fig. S5 *B* and *C*). These results further suggest that SFK-dependent p-Dock180^{Y722} is critical for EGFRvIII-stimulated p-Akt, p-Erk1/2, Rac1 activity, and cell migration in glioblastoma cells.

Coexpression of EGFRvIII, p-Dock180^{Y722} and pan-p-Src^{Y418} in Clinical Glioblastoma Specimens Correlates with an Extremely Poor Prognosis. We performed immunohistochemical (IHC) analysis using antibodies against p-Dock180^{Y722}, EGFRvIII, or p-SrcY^{418} (also detects p-Y of other SFKs) on a cohort of 124 clinical glioblastoma specimens with identifiable central and invasive regions (11). As shown in Table S1, EGFRvIII protein was detected by the specific anti–EGFRvIII-antibody DH8.3 (16) in 36 of 69 GBM (WHO grade IV, 52.2%) and 5 of 26 WHO grade II (19.2%), and 5 of 29 WHO grade III (17.2%) glioblastoma samples, similar to the frequency of EGFRvIII overexpression in clinical GBMs (2). Next, we stained these 46 EGFRvIII-positive tumors and an additional 11 EGFRvIII-negative samples. As shown in Tables S1 and S2, the majority of EGFRvIII-positive tumors demonstrated the presence of p-Dock180^{Y722} and pan-p-Src^{Y418}. Additionally, coexpression of EGFRvIII, p-Dock180^{Y722} and pan-p-Src^{Y418} was found in tumor cells within the invasive areas, as well as in the central regions (Tables S1–S3). An example is shown in Fig. 6*A*, where EGFRvIII was detected in both invasive (Fig. 6*Aa*) and central regions (Fig. 6*Ad*) in a GBM specimen. Interestingly, both pan p-Src^{Y418} and p-Dock180^{Y722} were also expressed in the majority of EGFRvIII-positive tumor cells in invasive and central regions of clinical WHO grade IV and II–III specimens (Fig. 6*A*, *b*, *c*, *e*, and *f*, Fig. S6, and Table S1). In contrast, EGFRvIII, p-Src^{Y418} and p-Dock180^{Y722} were not detected in normal brain tissues. Spearman's rank correlation analysis of expression levels of EGFRvIII and p-Dock180^{Y722} in all of these IHC-stained clinical specimens showed correlation coefficients between border vs. border regions as 0.9000 ($P < 0.05$), center vs. center regions as 0.9747 ($P < 0.05$), and invasive vs. invasive areas as 0.8721 ($P < 0.05$), respectively (Tables S2 and S3).

To further validate these findings, we examined expression of EGFRvIII, p-Src^{Y418}, and p-Dock180^{Y722} in a separate and independent cohort of 38 clinical GBM specimens by IB analyses. As shown in Fig. 6*B*, overexpression of EGFR and EGFRvIII was detected in 10 of 38 (26.3%) GBMs, whereas EGFR was overexpressed in an additional two GBMs, corroborating with the genetic analyses using fluorescent in situ hybridization. Dock180 was expressed at high levels in 25 of 38 GBMs, whereas pan-p-Src^{Y418} was also found in 27 of 38 tumors. Significantly, p-Dock180^{Y722} was coexpressed with pan-p-Src^{Y418} in 7 of 10 EGFR/EGFRvIII-expressing GBMs (tumors 2, 5, 11, 12, 15, 33, and 38), suggestive of the presence of activated EGFR/EGFRvIII-SFK-Dock180-Rac1 signaling in these GBMs. Additionally, Kaplan-Meier analyses showed that in these two independent cohorts, patients with high expression of EGFRvIII or p-Dock180^{Y722} have a shorter overall survival compared with those with low expression of EGFRvIII or p-Dock180^{Y722} (Fig. S7 *A* and *B*). In these cases, a statistically significant correlation was found between worse prognosis of patients with high expression of p-Dock180^{Y722} compared with low expression in the cohort that were analyzed by IHC staining (Fig. S7*A*). When combining the expression status of EGFRvIII and p-Dock180^{Y722} in the analyses, a statistically significant worse prognosis was apparent in glioblastomas with high expression of both proteins compared with those with low expression in both cohorts (Fig. 6*C*). Of note, compared with prognosis of glioblastomas with individual high expression of either EGFRvIII or p-Dock180^{Y722}, the better prognosis value of high expression of both proteins did not appear as drastic as we anticipated. However, this is probably because of the fact that overexpression of EGFRvIII is already a strong prognosis marker for malignant glioblastomas (1, 3) and a relative small number of cases (38 GBM samples) examined by IB analyses. Taken together, these data suggest that p-Dock180^{Y722} could be an independent, as well as an additional, clinically useful marker in the diagnosis and assessment of outcome in GBM with EGFRvIII overexpression.

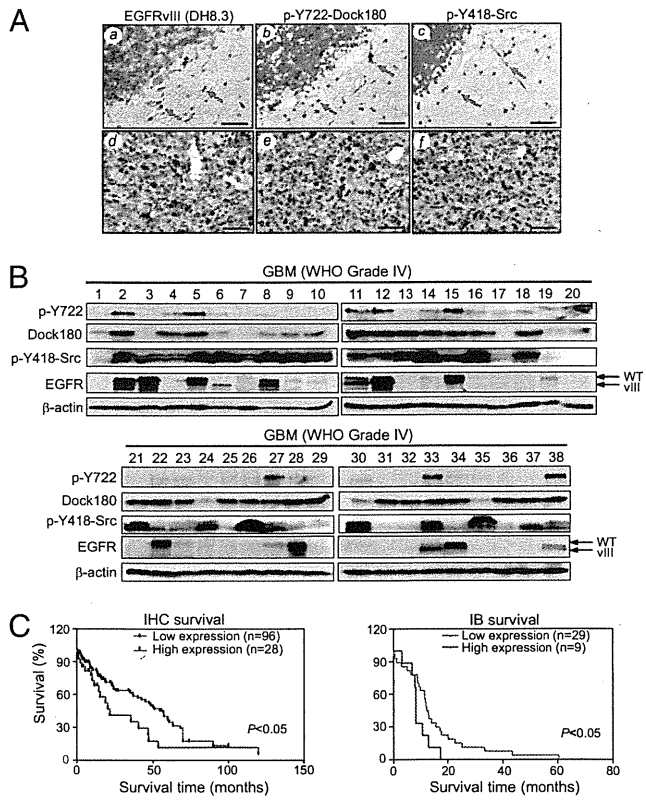

Fig. 6. Coexpression of p-Dock180^{Y722}, EGFRvIII and p-Src^{Y418} correlates with an extremely poor prognosis in patients with glioblastomas. (*A*) IHC analysis. A total of 57 specimens that express EGFRvIII and/or p-Dock180^{Y722} and p-Src^{Y418} are listed in Table S1. Representative images of GBM (grade IV) tissue stained by anti-EGFRvIII (*a* and *d*), anti–p-Src^{Y418} (*b* and *e*), and anti–p-Dock180^{Y722} (*c* and *f*) antibodies. Arrows, positive staining for EGFRvIII, p-Src^{Y418}, and p-Dock180^{Y722}. (Scale bars, 50 μm.) (*B*) IB analysis of a separate and independent cohort of 38 snap-frozen GBM specimens. Dock180 and β-actin were used as loading controls. (*C*) Kaplan-Meier curves with long-rank analyses for patients with high EGFRvIII/p-Dock180^{Y722}–expressing tumors (red line) versus low-expression tumors (blue line) of two separate cohorts of glioblastomas examined in *A* and *B*. *P* values were determined by using the log-rank test. Black bars, censored data. Data represent three independent experiments with similar results.

Discussion

In this study, we report that SFK-dependent p-Dock180^{Y722} mediates downstream EGFRvIII-signaling and glioblastoma growth and invasion. This study highlights four important points. First, Dock180 is required for EGFRvIII-stimulated glioblastoma cell migration and survival in vitro. Second, EGFRvIII induces a specific p-Y of Dock180 at Y722 and mutation of this p-Y site inhibits EGFRvIII-promoted glioblastoma cell migration and survival in vitro and tumor growth and invasion in vivo. Third, SFKs, Src, Fyn, and Lyn mediate EGFRvIII induction of phosphorylation of Dock180^{Y722} in glioblastoma cells stimulating tumorigenesis. Fourth, p-Dock180^{Y722} and p-Src^{Y418} are coexpressed with EGFRvIII in clinical glioblastoma specimens. Coexpression of EGFRvIII, p-Dock180^{Y722} and p-Src^{Y418} is correlated with an extremely poor prognosis in patients with glioblastomas. Taken together, our results suggest that SFK activation of p-Dock180^{Y722}-Rac1 signaling plays a critical role in EGFRvIII-driven glioblastoma tumorigenesis.

GEFs couple RTKs to Rac1 (9) and Dock180 is a downstream effector of EGFR-mediated cell migration in *Drosophila* (10). Here, we show that EGFRvIII induces SFKs-dependent p-Dock^{Y722}, thereby activating Rac1-signaling and promoting glioblastoma cell growth, survival, and invasion. Rac1 is downstream

of Dock180 (8) and modulates cell growth, survival, and motility (17). Consistent with this finding, inhibition of Dock180 by siRNA knockdown, overexpression of a Dock180^{Y722F} mutant, or suppression of SFKs impaired EGFRvIII-stimulated Rac1 activity and tumorigenesis. Moreover, EGFRvIII also activates the PI3K-Akt and MAPK pathways (3, 4) and induces a cytokine circuit that stimulates EGFR-signaling in neighboring tumor cells (18). Separate disruption of these downstream pathways inhibits EGFRvIII function, underscoring the heterogeneity of clinical glioblastomas. This heterogeneity is also illustrated by the fact that activated p-Src^{Y418} is detected in all 38 clinical glioblastoma samples, whereas EGFRvIII and p-Dock180^{Y722} are only expressed in 8 of 38 specimens. Similarly, in a total of 124 clinical glioblastoma specimens analyzed by IHC, p-Dock180^{Y722} and p-Src^{Y418} were not detected in a number of tumors that express EGFRvIII, suggesting that other signaling pathways are also involved in EGFRvIII-driven tumorigenesis. The heterogeneity of glioblastomas involved p-Y of Dock180 is further demonstrated by our recent study, showing that a Src-dependent p-Y of Dock180 mediates PDGFRα, another RTK that is often overexpressed in proneural subtype of human glioblasotmas (1–3), and promoted glioblastoma tumorigenesis. Moreover, PDGFRα/Src-induced p-Y of Dock180 is at another tyrosine residue of Dock180 (19), indicating a distinct signaling from PDGFRα/Src. Taken together, our results show that SFK-dependent p-Y of Dock180 mediates EGFRvIII and PDGFRα stimulation of Rac1 signaling, cell growth, survival, and invasion in glioblastomas.

Src, Lyn, and Fyn are expressed in clinical glioblastoma samples and EGFRvIII-expressing glioblastoma cells. Inhibition of Src, Lyn, or Fyn attenuated EGFRvIII-promoted tumorigenesis and invasion (13, 14). Our data are consistent with and extend these findings. We found that Src directly induces phosphorylation of Dock180^{Y722} and interaction of Dock180 with Rac1 in vitro and in glioblastoma cells. Moreover, inhibition of Src, Lyn, and Fyn by pharmacological inhibitors or shRNA knockdown reduces EGFRvIII-induced p-Dock180^{Y722}, Rac1 signaling and migration of glioblastoma cells. Coexpression of p-Dock180^{Y722}, EGFR, and EGFRvIII and p-Src^{Y418} in clinical glioblastoma tumor specimens correlates with an extremely poor prognosis. Therefore, our results integrate SFK-activated p-Dock180^{Y722}-Rac1 signaling in EGFRvIII-driven tumorigenesis.

It has been postulated that nonstimulated Dock180 assumes an inhibitory configuration in which the SH3 domain folds back and interacts with DHR-2 domain, preventing access of Rac1. Upon ELMO1 binding, folded Dock180 is opened to allow Rac1 binding to the DHR-2 domain (8). Similarly, the N terminus of a Rho GEF Vav1 interacts with its Dbl homology (DH) domain, thereby inhibiting GTPase binding (7). Moreover, a Src-induced p-Y of Vav1 at its N terminus opens the DH domain for Rac1 binding (7). Our data are consistent with this mechanism. We show that SFK-dependent p-Dock180^{Y722} is required for Dock180 activation of Rac1, thereby mediating EGFRvIII-promoted tumorigenesis. However, Y722 is not located in the identified functional domains but at the boundary of a helix/coil configuration in the DHR-1/DHR-2 interdomain of Dock180 (20). With the helix/coil repeats of the interdomain, the DHR-1 domain is brought into close apposition with DHR-2 and Rac1, bringing the membrane binding elements of DHR-1 and Rac1 into the same coplanarity, thereby enabling simultaneous membrane association of the ELMO1-Dock180-Rac1 complex. Additionally, a Dock180-Rac1 dimer is formed that binds to the membrane (20). Therefore, SFK-induced p-Y722 could be critical for the interdomain of Dock180 that holds DHR-1 adjacent to DHR-2 to form a dimeric complex and to achieve the activation of Rac1.

In summary, our data connect the sustained activation of EGFRvIII and SFKs to the p-Dock180^{Y722} that stimulates Rac1 signaling and malignant behavior of human glioblastoma cells. This unique link is underscored by coexpression of EGFRvIII, p-Src^{Y418} and p-Dock180^{Y722} in clinical glioblastoma specimens and association with extremely poor prognoses. Because activation of EGFRvIII and SFKs renders an aggressive glioblastoma phenotype and the induced p-Y of Rho GEF is a common mechanism that activates Rac1 signaling, our results suggest that targeting the EGFRvIII-SFK-Dock180-Rac1 pathway could offer hope in treating malignant glioblastomas with EGFRvIII overexpression.

Materials and Methods

For descriptions of cell lines, cell cultures, reagents, antibodies, DNA constructs, IB and IP, purification of recombinant proteins, in vitro Src tyrosine phosphorylation, pull-down assays of the binding of Dock180 with Rac1, and statistical analysis, see *SI Materials and Methods*. Experiments using animals were performed using a protocol that was reviewed and approved by the University of Pittsburgh Institutional Animal Care and Use Committee. Studies using human tissues were reviewed and approved by the Institutional Review Board involving Human Subjects at the University of Pittsburgh, Pittsburgh, PA.

ACKNOWLEDGMENTS. We thank M. Matsuda, S. Courtneidge, R. Pieper, E. van Meir, and Y. Zhou for providing reagents. This work was supported by National Institutes of Health Grants CA130966 (to S.-Y.C.) and CA102583 (to K.V.); a grant from the James S. McDonnell Foundation (to B.H.); a grant from the Pennsylvania Department of Health, and Innovative Research Scholar Awards (to S.-Y.C. and B.H.); Mayo Specialized Program of Research Excellence Grants CA108961 (to J.N.S.), CA106429 (to C.K.T.), and CA95616 (to W.K.C., and F.B.F.); Grant HL070561 and the National Basic Research Program of China Grant 2011CB964801 (to T.C.); an award from the Goldhirsh Foundation (to F.B.F.); and a Clinical Fellowship from the Victorian Cancer Center (to T.G.J.). W.K.C. is a fellow of the National Foundation for Cancer Research. This project used the shared facilities at the University of Pittsburgh Cancer Institute that were supported in part by National Institutes of Health Grant P30CA047904.

1. Van Meir EG, et al. (2010) Exciting new advances in neuro-oncology: The avenue to a cure for malignant glioma. *CA Cancer J Clin* 60:166–193.
2. Cancer Genome Atlas Research Network (2008) Comprehensive genomic characterization defines human glioblastoma genes and core pathways. *Nature* 455: 1061–1068.
3. Furnari FB, et al. (2007) Malignant astrocytic glioma: Genetics, biology, and paths to treatment. *Genes Dev* 21:2683–2710.
4. Huang PH, Xu AM, White FM (2009) Oncogenic EGFR signaling networks in glioma. *Sci Signal* 2:re6.
5. Nishikawa R, et al. (1994) A mutant epidermal growth factor receptor common in human glioma confers enhanced tumorigenicity. *Proc Natl Acad Sci USA* 91: 7727–7731.
6. Cai XM, et al. (2005) Protein phosphatase activity of PTEN inhibited the invasion of glioma cells with epidermal growth factor receptor mutation type III expression. *Int J Cancer* 117:905–912.
7. Rossman KL, Der CJ, Sondek J (2005) GEF means go: Turning on RHO GTPases with guanine nucleotide-exchange factors. *Nat Rev Mol Cell Biol* 6:167–180.
8. Côté JF, Vuori K (2007) GEF what? Dock180 and related proteins help Rac to polarize cells in new ways. *Trends Cell Biol* 17:383–393.
9. Schiller MR (2006) Coupling receptor tyrosine kinases to Rho GTPases—GEFs what's the link. *Cell Signal* 18:1834–1843.
10. Duchek P, Somogyi K, Jékely G, Beccari S, Rørth P (2001) Guidance of cell migration by the *Drosophila* PDGF/VEGF receptor. *Cell* 107:17–26.
11. Jarzynka MJ, et al. (2007) ELMO1 and Dock180, a bipartite Rac1 guanine nucleotide exchange factor, promote human glioma cell invasion. *Cancer Res* 67:7203–7211.
12. Hu B, et al. (2009) ADP-ribosylation factor 6 regulates glioma cell invasion through the IQ-domain GTPase-activating protein 1-Rac1-mediated pathway. *Cancer Res* 69:794–801.
13. Stettner MR, et al. (2005) Lyn kinase activity is the predominant cellular Src kinase activity in glioblastoma tumor cells. *Cancer Res* 65:5535–5543.
14. Lu KV, et al. (2009) Fyn and Src are effectors of oncogenic epidermal growth factor receptor signaling in glioblastoma patients. *Cancer Res* 69:6889–6898.
15. Giannini C, et al. (2005) Patient tumor EGFR and PDGFRA gene amplifications retained in an invasive intracranial xenograft model of glioblastoma multiforme. *Neuro-oncol* 7:164–176.
16. Jungbluth AA, et al. (2003) A monoclonal antibody recognizing human cancers with amplification/overexpression of the human epidermal growth factor receptor. *Proc Natl Acad Sci USA* 100:639–644.
17. Burridge K, Wennerberg K (2004) Rho and Rac take center stage. *Cell* 116:167–179.
18. Inda MM, et al. (2010) Tumor heterogeneity is an active process maintained by a mutant EGFR-induced cytokine circuit in glioblastoma. *Genes Dev* 24:1731–1745.
19. Feng H, et al. (2011) Activation of Rac1 by Src-dependent phosphorylation of Dock180Y1811 mediates PDGFRα-stimulated glioma tumorigenesis in mice and humans. *J Clin Invest* 121:4670–4684.
20. Premkumar L, et al. (2010) Structural basis of membrane targeting by the Dock180 family of Rho family guanine exchange factors (Rho-GEFs). *J Biol Chem* 285: 13211–13222.

J Neurosurg 119:1331–1339, 2013

Cadherin 13 overexpression as an important factor related to the absence of tumor fluorescence in 5-aminolevulinic acid–guided resection of glioma

Laboratory investigation

Tomonari Suzuki, M.D.,[1] Satoru Wada, Ph.D.,[2,4] Hidetaka Eguchi, Ph.D.,[2,3] Jun-ichi Adachi, M.D., Ph.D.,[1] Kazuhiko Mishima, M.D., Ph.D.,[1] Masao Matsutani, M.D., Ph.D.,[1] Ryo Nishikawa, M.D., Ph.D.,[1] and Masahiko Nishiyama, M.D., Ph.D.[2,3,5]

[1]Department of Neuro-Oncology/Neurosurgery, International Medical Center, Hidaka; [2]Project Division and [3]Division of Translational Research, Research Center for Genomic Medicine, Saitama Medical University, Hidaka; [4]Information Technology Center, Saitama Medical University, Moroyama; and [5]Department of Molecular Pharmacology and Oncology, Gunma University Graduate School of Medicine, Maebashi, Japan

Object. Gliomas contain aggressive malignant cancer, and resection rate remains an important factor in treatment. Currently, fluorescence-guided resection using orally administered 5-aminolevulinic acid (5-ALA) has proved to be beneficial in improving the prognosis of patients with gliomas. 5-ALA is metabolized to protoporphyrin IX (PpIX) that accumulates selectively in the tumor and exhibits strong fluorescence upon excitation, but glioma cells do not always respond to 5-ALA, which can result in incomplete or excessive resection. Several possible mechanisms for this phenomenon have been suggested, but they remain poorly understood. To clarify the probable mechanisms underlying the variable induction of fluorescence and to improve fluorescence-guided surgery, the authors searched for key negative regulators of fluorescent signal induced by 5-ALA.

Methods. A comprehensive gene expression analysis was performed using microarrays in 11 pairs of tumor specimens, fluorescence-positive and fluorescence-negative tumors, and screened genes overexpressed specifically in fluorescence-negative tumors as the possible candidates for key negative regulators of 5-ALA–induced fluorescence. The most possible candidate was selected through annotation analysis in combination with a comparison of expression levels, and the relevance of expression of the selected gene to 5-ALA–induced fluorescence in tumor tissues was confirmed in the quantified expression levels. The biological significance of an identified gene in PpIX accumulation and 5-ALA–induced fluorescence was evaluated by in vitro PpIX fluorescence intensity analysis and in vitro PpIX fluorescence molecular imaging in 4 human glioblastoma cell lines (A1207, NMCG1, U251, and U373). Knockdown analyses using a specific small interfering RNA in U251 cells was also performed to determine the mechanisms of action and genes working as partners in the 5-ALA metabolic pathway.

Results. The authors chose 251 probes that showed remarkably high expression only in fluorescent-negative tumors (median intensity of expression signal > 1.0), and eventually the cadherin 13 gene *(CDH13)* was selected as the most possible determinant of 5-ALA–induced fluorescent signal in gliomas. The mean expression level of *CDH13* in the fluorescence-negative gliomas was statistically higher than that in positive ones ($p = 0.027$), and knockdown of *CDH13* expression enhanced the fluorescence image and increased the amount of PpIX 13-fold over controls ($p < 0.001$) in U251 glioma cells treated with 5-ALA. Comprehensive gene expression analysis of the *CDH13*-knockdown U251 cells demonstrated another two genes possibly involved in the PpIX biosynthesis: ATP-binding cassette transporter *(ABCG2)* significantly decreased in the *CDH13* knockdown, while oligopeptide transporter 1 *(PEPT1)* increased.

Conclusions. The cadherin 13 gene might play a role in the PpIX accumulation pathway and act as a negative regulator of 5-ALA–induced fluorescence in glioma cells. Although further studies to clarify the mechanisms of action in the 5-ALA metabolic pathway would be indispensable, the results of this study might lead to a novel fluorescent marker able to overcome the obstacles of existing fluorescence-guided resection and improve the limited resection rate.
(http://thejns.org/doi/abs/10.3171/2013.7.JNS122340)

Key Words • **5-aminolevulinic acid** • **glioma** • **cadherin 13** • **photodynamic diagnosis**

Abbreviations used in this paper: ABC = ATP-binding cassette; *ACTB* = actin, beta; ALAD = aminolevulinate dehydratase; ALAS = aminolevulinate synthase; ATP = adenosine 5′-triphosphate; CDH13 = cadherin 13; CPOX = coproporphyrinogen oxidase; DMEM = Dulbecco modified Eagle medium; *FECH* = ferrochelatase; GAPDH = glyceraldehyde 3-phosphate dehydrogenase; HMBS = hydroxymethylbilane synthase; PEPT1 = peptide transporter 1; PpIX = protoporphyrin IX; PPOX = protoporphyrinogen oxidase; RT-PCR = reverse transcription polymerase chain reaction; SAM = significance analysis of microarrays; siRNA = small interfering RNA; UROD = uroporphyrinogen decarboxylase; UROS = uroporphyrinogen III synthase; 5-ALA = 5-aminolevulinic acid.

Gliomas contain aggressive, malignant forms of cancer.[9,14] Despite improvement in chemoradiotherapy, high-grade glioma is often fatal. The effect of current standard therapy using temozolomide with radiation for glioblastoma, the most malignant type of glioma, is marginal, and the median survival time is merely 1.3 years.[29]

Surgery continues to be the mainstay treatment for gliomas. The resection rate is a key determinant of prognosis,[13,24] with the most difficult obstacle being the unclear tumor margin during resection. To remove tumor

without damaging the normal adjacent tissues, Stummer et al. first attempted photodynamic diagnostic surgery using 5-aminolevulinic acid (5-ALA) in 1998 and demonstrated that normal brain tissue revealed no porphyrin fluorescence, whereas tumor tissue was distinguished by bright red fluorescence due to the response of glioma to 5-ALA.[28] Currently, fluorescence-guided resection is widely applied,[18,20,25,33] and it has certainly improved the resection rate and prognosis for gliomas. A randomized, controlled, Phase III trial demonstrated that the overall resection rate (65% vs 36%, respectively) and 6-month progression-free survival rate (41% vs 21%, respectively) were significantly improved in the 5-ALA assigned group compared with the control group.[27] Nevertheless, it is now widely recognized that glioma cells do not always respond to 5-ALA even in the same patient, and the heterogeneous response can cause an incomplete or excessive resection in some cases. Several possible mechanisms for this phenomenon have been suggested, but they remain poorly understood.[4,7,30,32]

5-ALA is metabolized to the protoporphyrinogen IX in mitochondria via the heme biosynthesis pathway and is finally converted to protoporphyrin IX (PpIX) by a protoporphyrinogen IX oxidase. The synthesized PpIX densely accumulates in the tumor cells and shows bright fluorescence upon excitation with blue light. Various transporters, or factors, have been suggested to be involved in the PpIX biosynthesis pathways, including ferrochelatase *(FECH)* in tumor cells.[32] None of these factors alone, however, has proved consistently critical in the mechanisms of PpIX accumulation,[11] so more important mechanisms and key regulators might exist in the PpIX biosynthesis pathways and the induction mechanism of fluorescence by 5-ALA.

In this study, we attempted to select possible determinants of the fluorescent signal induced by 5-ALA using comprehensive gene expression analysis to clarify the probable mechanisms underlying the variable induction of fluorescence.

Methods

Cell Lines

Four human glioblastoma cell lines (A1207, NMCG1, U251, and U373) were used in this study. The U251 cells were obtained from American Type Culture Collection; A1207 and U373 were kindly donated by Dr. Webster K. Cavenee of the Ludwig Institute for Cancer Research; and NMCG1 was kindly provided by Dr. T. Todo at the University of Tokyo. All tumor cells were cultured in Dulbecco modified Eagle medium (DMEM) containing 10% fetal bovine serum and maintained at 37°C in air containing 5% CO_2.

Clinical Samples

A total of 70 patients with diagnosed brain tumors were enrolled in this study between March 2006 and January 2009. Among these 70 patients, 16 with gliomas were eligible for the study according to the study criteria, which were patients with a tumor containing both positive and negative fluorescence signal sites induced by 5-ALA. Of the 16 gliomas, 11 were diagnosed as glioblastomas, and histopathological diagnoses of the other 5 gliomas were anaplastic astrocytoma, anaplastic ependymoma, anaplastic oligodendrogliomas, oligoastrocytoma, and pilocytic astrocytoma. Patients were orally administered 20 mg/kg of 5-ALA (Cosmo Bio) 4 hours before the operation, and fluorescence was determined using a semiconductor laser with a VLD-M1 spectrometer (M&M Co., Ltd.) at surgery. Based on the fluorescent signals, we collected tissue samples from each patient at surgery (both fluorescence-positive and fluorescence-negative tumor sites). All samples were immediately frozen and stored at −80°C until microarray and real-time reverse transcription polymerase chain reaction (RT-PCR) analyses. The study was approved by the Ethics Committee at Saitama Medical University, and written informed consent was obtained from all patients.

RNA Isolation and Quality Determination

Total RNA was extracted from frozen tissue samples and glioblastoma cells using the RNA Nucleospin RNAII kit (Macherey-Nagel) according to the manufacturer's protocols. The quality of total RNA was determined with a 2100 Bioanalyzer (Agilent Technologies) to check the RNA integrity number; we chose samples with an RNA integrity number greater than 7.0.

DNA Microarray Analysis

Comprehensive gene expression analysis was performed using the Agilent Whole Human Genome Oligo Microarray Kit (4 × 44K; Agilent Technologies) as previously reported.[22] The scanned image data were analyzed with Agilent Feature Extraction software (version 9.5, Agilent Technologies), and gene expression signals were normalized using GeneSpring GX (Agilent Technologies) and further analyzed using Spotfire software (Tibco Software).

Statistical Methods to Select Candidate Genes

Initially, the analytical probes were determined according to 2 criteria: the probes had an observed expression intensity greater than 0 in over half of the samples and had a coefficient variation value greater than 0.3. Among the analytical probes, the candidates, which were differently expressed between 5-ALA–induced fluorescence-positive and fluorescence-negative samples, were selected. To do so, we referred to the fold-change values in the expression intensity and further used the significance analysis of microarrays (SAM) statistical method.[34] In the SAM method, the differences were ranked, and a small positive constant was added to the denominator of the gene-specific t-test to omit genes with low expression values. Multiple comparison of PpIX fluorescence intensity was conducted using 1-way ANOVA, followed by the Dunnett test, using U373 cells as the referent. Statistical calculations were performed using "R" statistical software (http://www.r-project.org/) with the "samr" package.[34] Ingenuity Pathways Analysis (Ingenuity Systems) was used in screening candidate genes for 5-ALA–induced PpIX accumulation- and cancer-related factors.[15]

Real-Time RT-PCR

To quantify gene expression level, real-time RT-PCR was conducted using total RNA (1 μg) extracted from each cell line or tumor tissue, according to the manufacturer's instructions.[17] Primers and probes for each gene were designed using the Probe Finder software in the Universal Probe Library Assay Design Center (Roche). The expression level of each gene was normalized as a ratio to that of actin beta *(ACTB)* in vivo, and hypoxanthine phosphoribosyltransferase 1 *(HPRT1)* in in vitro experiments.

Cadherin 13 Knockdown Experiment

To downregulate endogenous cadherin 13 *(CDH13)* expression in U251, we used 2 Stealth small interfering RNAs (siRNAs) targeting *CDH13* that had been custom-synthesized by Invitrogen. Sequences of the 2 siRNAs are 1): sense primer 5′-TATTGTTGATCTTGGAGATCT TCCA-3′ and antisense primer 5′-TGGAAGATCTCCA AGATCAACAATA-3′; and 2): sense primer 5′-ATAAA CAGCGATTACTTCTCTGTCC-3′ and antisense primer 5′-GGACAGAGAAGTAATCGCTGTTTAT-3′.

Stealth siRNA negative control duplexes (Invitrogen) whose guanine-cytosine content was close to that of each duplex siRNA were used as controls. The U251 cells were seeded in 24-well plates at a density of 2×10^4 cells/well, and then transfected with the Stealth or control siRNA using Lipofectamine RNAiMAX transfection agent (Invitrogen) according to the manufacturer's recommended procedure.

Western Blot Analysis

Western blot analysis was performed to confirm *CDH13* levels using anti-*CDH13* polyclonal antibody (ab50846; Abcam). Whole cell lysates were extracted from U251 72 hours after transfection with Stealth or control siRNA, separated using 15% sodium dodecyl sulfate polyacrylamide gels, and transferred to a polyvinylidene difluoride membrane. The membranes were incubated with *CDH13* antibody or glyceraldehyde 3-phosphate dehydrogenase (*GAPDH*, ab8245; Abcam) as an internal control. Immunoreactive proteins were visualized using horseradish peroxidase–linked anti–rabbit (W401B; Promega) or anti–mouse immunoglobulin (NA931; GE Healthcare) using the ECL-Plus system (GE Healthcare) and luminoimage analyzer (LAS-4000 mini, FujiFilm Corp.).

In Vitro PpIX Fluorescence Molecular Imaging

After incubation in serum-free DMEM containing 5-ALA solution (final concentration 400 μM) for 6 hours at 37°C, PpIX-specific fluorescence in cells was captured by fluorescence microscopy (Olympus IX71 inverted microscope) and a digital camera (Olympus DP71) under the same exposure times. Intracellular PpIX was excited at a wavelength of 407 nm, and molecular images were collected in the red channel through 655-nm long-pass filters.

In Vitro PpIX Fluorescence Intensity Analysis

The A1207, NMCG1, U373, and U251 cells (5×10^5 cells) were incubated with serum-free DMEM for 12 hours to adhere tightly to culture dishes and then exposed to 5-ALA (final concentration 400 μM) for 6 hours at 37°C. The cells were collected, resuspended in 100-μl extraction solution (50 mM Tris-HCl, pH 7.5; 100 mM NaCl; 2.5% Triton X-100), shaken for 1 minute at room temperature, and centrifuged at 15,000 rpm for 5 minutes. The supernatant was transferred into 300 μl of ethyl acetate and glacial acetic acid solution (V/V, 2:1). After 1 minute of vigorous shaking, 300 μl of 0.6 M NaOH was added to the supernatant and centrifuged at 15,000 rpm for 2 minutes. The upper phase was dissolved in 300 μl of 0.5 M HCl and centrifuged at 15,000 rpm for 2 minutes, and then the lower phase was collected and read for PpIX fluorescence using the ARVO MX plate reader (Perkin-Elmer).

In *CDH13* knockdown experiments, U251 cells were incubated with *CDH13* siRNA no. 1 to attenuate *CDH13* expression in 24-well plates at 37°C for 72 hours, and then the media in each well were replaced with serum-free DMEM containing 5-ALA solution. After the 6-hour incubation, PpIX was extracted and PpIX fluorescence intensity was measured using the protocol detailed above. In *CDH13* knockdown experiments, the fluorescence intensity of PpIX was normalized as a ratio to total protein content to correct variations in the number of cells in each well.

Results

Selection of Genes Related to 5-ALA–Induced Tumor Fluorescence Signal

We used a total of 22 samples collected from 11 of the 16 patients as analytical grade tumors. Of these 11 patients, 4 were female and 7 were male; the median age was 45 years old (range 2–80 years old). The tumors included 7 glioblastomas, 1 anaplastic astrocytoma, 1 anaplastic ependymoma, 1 oligoastrocytoma, and 1 pilocytic astrocytoma, and all of the tumors were displayed as strongly enhanced rings and/or solid tumor masses with surrounding edema using preoperative Gd-enhanced MRI.

To screen genes overexpressed only in 5-ALA–induced fluorescence-negative tumors, we performed comprehensive gene expression analysis using microarrays in 11 pairs of tumor specimens showing and not showing 5-ALA–induced fluorescence. A total of 5606 probes were evaluated for their ability to analyze expression levels, and 2 statistical methods (a fold-change value analysis and the SAM method) provided 500 and 2000 possible probes as candidates, respectively. Among those that fulfilled both of these criteria, we chose 251 probes that showed remarkably high expression only in fluorescent-negative tumors (median intensity of expression signal > 1.0). We then selected 68 cancer-related genes (80 probes) as functionally annotated by the Ingenuity Pathways Analysis Knowledge Base, and finally pinpointed *CDH13*, known as a tumor suppressor gene,[31] as the most likely determinant of a 5-ALA–induced fluorescence signal in glioma. In general, a tumor suppressor gene is related to the malignancy of a tumor, which is believed to be corre-

lated with a positive rate of 5-ALA–induced fluorescence signal.[6,21,26,27]

The relevance of *CDH13* expression to 5-ALA–induced fluorescence in tumor tissues was confirmed in the quantified expression levels. Real-time RT-PCR analysis followed by a paired t-test revealed that the expression level of *CDH13* was significantly higher in fluorescence-negative tumors (mean 0.09388, range 0.00135–0.34966) than in corresponding fluorescence-positive tumor tissues (mean 0.04610, range 0.00004–0.25442; $p = 0.027$), although the *CDH13* expression levels varied significantly among tumors (Fig. 1). The increased expression in fluorescence-negative tumors was observed in 8 of 11 pairs of tumor samples, but not in 3 pairs of tumor specimens with extremely low *CDH13* expression.

Significance of Selected Gene as a Determinant of 5-ALA–Induced Fluorescence Signal

Cadherin 13 might participate in the 5-ALA–induced fluorescence pathway. To evaluate its functional significance in the pathway, PpIX accumulation—the critical cause of bright fluorescence upon excitation with blue light—along with the *CDH13* expression was measured in 4 glioma cell lines (U373, U251, A1207, and NMCG1). The relative expression levels of *CDH13* in U251, A1207, and NMCG1 were 4.5-, 7.7-, and 17.1-fold, respectively, compared with U373 cells (Fig. 2). On the other hand, intensities of fluorescence by accumulated PpIX after exposure to 5-ALA were significantly lower in U251, A1207, and NMCG1 cells than in U373 cells ($p < 0.001$ for all 3, respectively, using the Dunnett test), although the fluorescence intensity in NMCG1 was not lower than that in A1207.

The results shown in NMCG1 encouraged us to perform *CDH13* knockdown experiments in U251 cells using specific siRNAs to elucidate the relevance of *CDH13* expression to 5-ALA–induced fluorescence. The knockdown experiments clearly demonstrated enhancement of 5-ALA–induced fluorescence associated with reduced expression of *CDH13*, both in the protein and mRNA levels (Fig. 3A–C). Furthermore, PpIX fluorescence intensity analysis revealed that *CDH13* knockdown caused an approximately 13-fold increase of PpIX accumulation (normalized by the amount of total protein) in U251 cells (Fig. 3D).

In general, knockdown of the tumor suppressor gene causes an increase in cell viability, which was confirmed also in *CDH13*: 3′(4,5-dimethylthiazol-2-yl)2,5-diphenyltetrazolium bromide assay after *CDH13* siRNA treatment demonstrated a significant increase in the number of viable cells in U251 after *CDH13* knockdown ($p < 0.001$).

Possible Role of CDH13 in PpIX Accumulation Pathway

Cadherin 13 may play some important role in accumulation of PpIX and proliferation in tumor cells, thereby relating to 5-ALA–induced fluorescence. To clarify the role of *CDH13* in the PpIX accumulation pathway, we at-

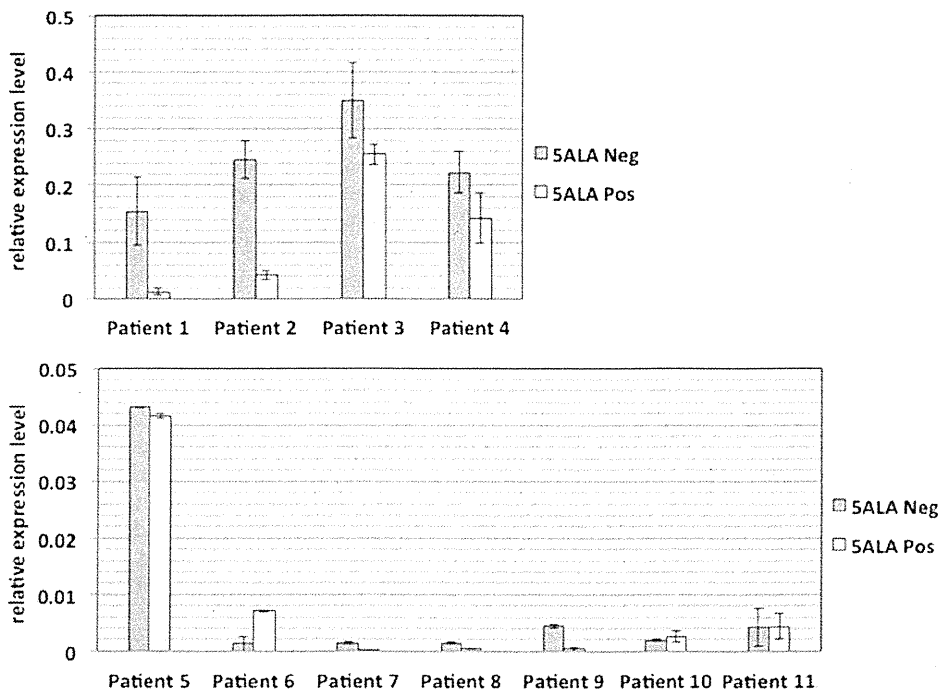

Fig. 1. Cadherin 13 expression levels and 5-ALA–induced fluorescence in glioma tissues. A total of 11 paired sets of tumor tissues, fluorescence-positive *(white bars)* and fluorescence-negative *(gray bars)* samples, were collected from 11 patients who had undergone 5-ALA–guided resection. The *CDH13* expression levels in tissue specimens were measured by real-time RT-PCR and normalized to *ACTB*. Because the expression levels varied significantly among tumors, 2 graphs were made **(upper and lower)** according to the relative expression level. Statistical differences in *CDH13* expression were analyzed using the paired t-test.

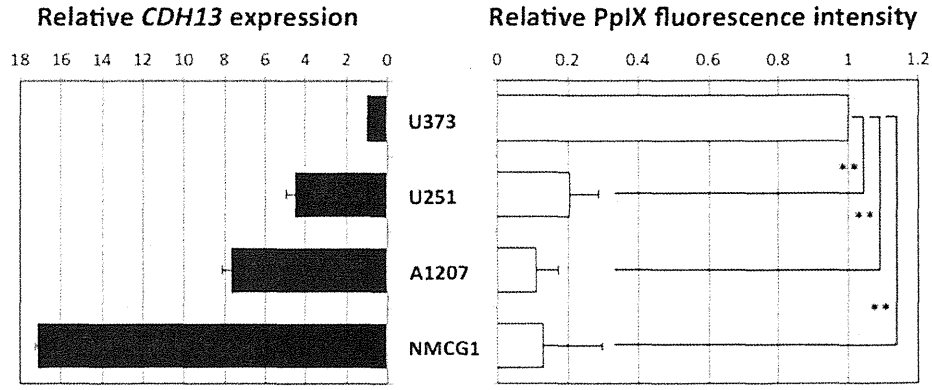

Fig. 2. Expression of *CDH13* and 5-ALA–induced PpIX accumulation in glioma cells. In 4 human glioma cell lines, *CDH13* expression **(left)** was analyzed using real-time RT-PCR and compared with 5-ALA–induced PpIX accumulation **(right)** measured using PpIX fluorescence intensity analysis. Both *CDH13* expression levels and PpIX fluorescence intensities were described as relative values to the mean value of those in U373. Data are expressed as mean ± SD, from 3 independent experiments. Multiple comparisons of PpIX fluorescence intensity were conducted using 1-way ANOVA, followed by the Dunnett test. ** $p < 0.001$.

tempted to find another important factor that was functionally related to *CDH13* in the PpIX accumulation pathway. Microarray analysis was performed on U251 cells treated with siRNA or control for 72 hours. Comparison of the gene expression data between cells transfected with control and *CDH13* siRNA no. 1 showed that 179 genes were significantly upregulated, while 237 were downregulated, in association with the *CDH13* knockdown. Among these, there were 2 possible genes that might be involved in the porphyrin biosynthesis: ATP-binding cassette transporter *ABCG2*, the pump for discharging PpIX out of cells, and *PEPT1*, which transports 5-ALA

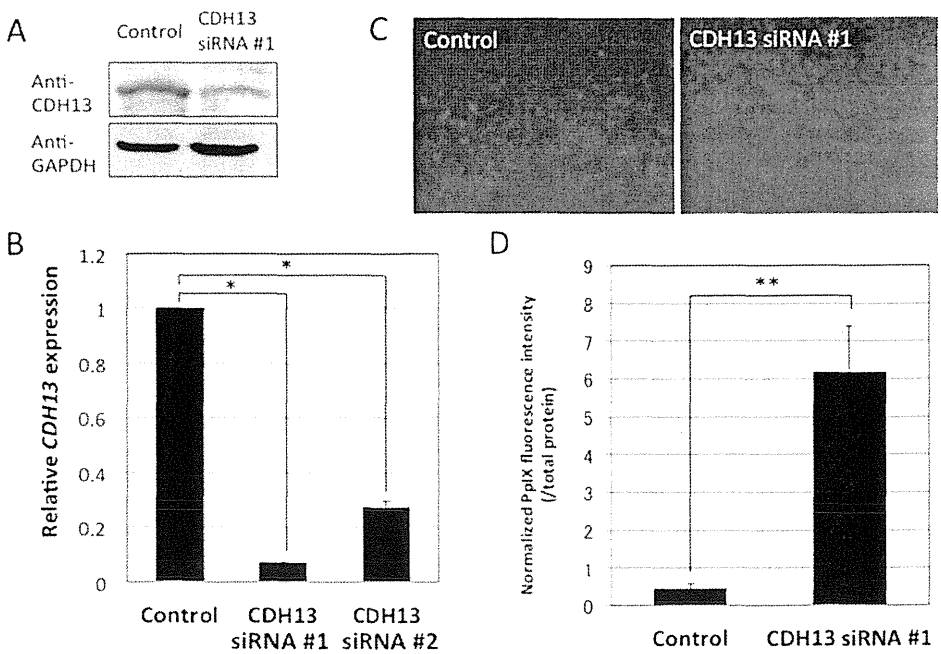

Fig. 3. Effect of *CDH13* knockdown on 5-ALA–induced PpIX accumulation and fluorescence in U251 cells. The *CDH13* knockdown experiments were performed in U251 cells to elucidate the relevance of *CDH13* expression to 5-ALA–induced fluorescence. The specific siRNAs (*CDH13* siRNA #1 and #2) successfully reduced CDH13 expression in both the protein **(A)** and mRNA levels **(B)**. The amount of CDH13 protein was measured at 72 hours after transfection of siRNA #1 into U251 cells. Glyceraldehyde 3-phosphate dehydrogenase is included as a loading control (A). The *CDH13* mRNA levels were measured by real-time RT-PCR 24 hours after transfection in U251 cells and are shown as relative value to the mean value of the control. Data are expressed as mean ± SD, from 3 independent experiments (B). Cadherin 13 knockdown increased 5-ALA–induced fluorescence in U251 cells treated with 5-ALA at a concentration of 400 μM for 6 hours, which was observed in both PpIX fluorescence molecular imaging **(C)** and PpIX fluorescence intensity analysis **(D)**. The 5-ALA–induced PpIX accumulation in *CDH13* knockdown cells was measured by PpIX fluorescence intensity analysis in 24-well plates, and the fluorescence intensity of PpIX was normalized to total protein content to correct any variation in the number of cells in each well. Data are presented as mean ± SD from 4 independent experiments (D). Statistical analysis was performed using the t-test. * $p < 0.05$, ** $p < 0.001$.

into the cells. The *ABCG2* expression levels in *CDH13* knockdown cells were 7.3% of the control with microarray analysis (Table 1), which was confirmed in the quantified expression levels measured by real-time RT-PCR ($p < 0.001$; Fig. 4). On the other hand, *CDH13* knockdown caused a 12.5-fold increase of *PEPT1* expression compared with the control (Table 1).

There are 10 other possible factors that have already been shown to be involved in porphyrin biosynthesis: ABC transporter *ABCB6*, aminolevulinate dehydratase *(ALAD)*, aminolevulinate synthase 1, 2 *(ALAS1, ALAS2)*, coproporphyrinogen oxidase *(CPOX)*, *FECH*, hydroxymethylbilane synthase *(HMBS)*, protoporphyrinogen oxidase *(PPOX)*, uroporphyrinogen decarboxylase *(UROD)*, and uroporphyrinogen III synthase *(UROS)*.[12] However, *CDH13* knockdown did not cause any significant alteration in expression levels of these factors (Table 1).

Discussion

In this study, *CDH13* was suggested to play some important roles in the PpIX accumulation pathway, indicating that it is a key regulator of 5-ALA–induced fluorescence in glioma cells. Despite several discrepant results, *CDH13* was shown to be overexpressed, mostly in 5-ALA–induced fluorescence-negative tumors, and related to the pathway of PpIX accumulation. The downregulation of *CDH13* expression facilitated PpIX accumulation through the regulation of important factors such as *PEPT1* and *ABCG2* in the PpIX accumulation pathway in glioma cells. Cadherin 13 thus could be a potent candidate molecule in the new approach to enhance 5-ALA–induced fluorescence in brain tumors, which might lead to improvement in 5-ALA–guided resection, and thus curative resection rates for gliomas.

Cadherin 13 is a member of the cadherin superfamily and is highly expressed in the nervous system.[31] A variety of studies have demonstrated the functional role of *CDH13* in cell proliferation, the cell cycle, and epigenetic silencing in cancer, and *CDH13* is now recognized as a tumor suppressor gene. *CDH13* is believed to suppress the development of neural cells[31] and induce G2 (premiotic phase) arrest in astrocytomas via p21.[8] The expression of *CDH13* is downregulated through methylation in breast, ovarian, and lung cancer,[2] is suggested as an early marker for lung cancer,[6] and is a potent predictor of poor prognosis in lung, ovarian, and esophageal cancers.[2] Despite numerous studies on tumor suppressor genes, this study may be the first to show the possible role of *CDH13* in PpIX biosynthesis pathways.

Protoporphyrin IX biosynthesis pathways have been intensively investigated for PpIX accumulation induced by 5-ALA, but the details remain unknown. Numerous studies have been conducted to elucidate the mechanisms and critical factors in the pathway. Recent studies demonstrated that *FECH* and *CPOX* might be included in PpIX biosynthesis pathways and accumulation of PpIX in gliomas;[30,32] more recently, downregulation of *ABCG2* was suggested as a cause of increased PpIX accumulation in colorectal and cervical cancers.[5] The mechanisms, however, are now recognized to be multifactorial, and so none of the factors have been established as the principal one in the pathway. With the exception of *ABCB2*, this study did not demonstrate any significant roles for *FECH* and *CPOX*, as well as other suggested factors such as *ABCB6*, *ALAD*, *ALAS1*, *ALAS2*, *HMBS*, *PPOX*, *UROD*, and *UROS* in porphyrin biosynthesis.[12]

Our study may be the first attempt to perform a nonhypothetical screening of novel and important regulators of 5-ALA–induced PpIX accumulation using comprehensive gene expression analysis. To reduce the selection bias—individual variability of the gene expression profiles caused by age, sex, and others—we selected 22 tumor samples from 11 patients for pair-wise comparison of gene expression between positive and negative signal samples. Then we employed 2 different statistical selection methods for candidate genes—fold-change and SAM statistical values—and found 68 genes selectively overexpressed in negative signal samples as final candidates for clinical application in the future. Among these,

TABLE 1: Influence of *CDH13* knockdown on gene expression related to PpIX biosynthesis pathways

Gene Symbol	Gene Name	Change of Gene Expression Caused by *CDH13* Knockdown	Expression Signal	
			CDH13 Knockdown Cells	Negative Control Cells
ABCB6	*ATP-binding cassette, sub-family B (MDR/TAP), member 6*	−0.292	1.65	1.94
ABCG2	*ATP-binding cassette, sub-family G (WHITE), member 2*	−3.777	−4.38	−0.6
ALAD	*aminolevulinate, dehydratase*	0.22	−1.49	−1.71
ALAS1	*aminolevulinate, delta-, synthase 1*	−0.482	0.43	0.91
ALAS2	*aminolevulinate, delta-, synthase 2*	0.02	−7.73	−7.75
CPOX	*coproporphyrinogen oxidase*	−0.218	−0.18	0.04
FECH	*ferrochelatase*	0.06	−0.12	−0.18
HMBS	*hydroxymethylbilane synthase*	−1.135	2.96	4.1
PEPT1	*oligopeptide transporter 1*	3.64	−3.52	−7.17
PPOX	*protoporphyrinogen oxidase*	0.097	1.41	1.31
UROD	*uroporphyrinogen decarboxylase*	0.095	4.9	4.8
UROS	*uroporphyrinogen III synthase*	−0.87	−1.17	−0.3

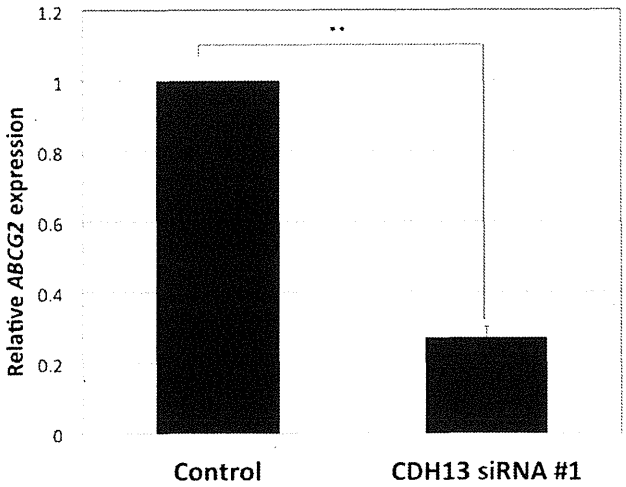

FIG. 4. Effects of *CDH13* knockdown on *ABCG2* expression in U251. The *ABCG2* mRNA levels were measured by real-time RT-PCR at 72 hours after transfection with *CDH13* siRNA #1. Expression of *ABCG2* is shown as relative value to the mean value in the control. Data are expressed as mean ± SD, from 3 independent experiments. Statistical analysis was performed using the t-test. ** $p < 0.001$.

we selected genes that were believed to be related to tumor progression because positive response to 5-ALA in fluorescence induction is suggested as being closely correlated with malignant grade of glioma.[6,21,26,27] The final candidate genes included only 1 tumor suppressor gene, *CDH13*, and the functional significance of *CDH13* as a negative regulator of 5-ALA–induced fluorescence was shown in in vitro experiments, so we believe that this selection approach can elucidate more detailed PpIX biosynthesis pathways.

We measured the amount of PpIX using fluorescence intensity analysis instead of direct PpIX measurement, thinking the former might have advantages in fluorescence quantification over other detection methods[10,16,23] Our results of the association between *CDH13* expression and amount of intracellular PpIX in cell lines and tumor specimens strongly suggested that the *CDH13* might act on PpIX accumulation. Results clearly demonstrated that *CDH13* siRNA caused an increase of PpIX accumulation and 5-ALA–induced fluorescence in glioma cells, suggesting that *CDH13* downregulation can improve the accuracy of PpIX fluorescence-guided discrimination of malignant cells. Even so, the mechanism or mechanisms of fluorescence augmentation by *CDH13* knockdown remains undetermined. Observed correlations of *CDH13* with PpIX accumulation and 5-ALA–induced fluorescence in tumor tissues were less robust as compared with those in tumor cells. This might be due to the technical issues of the existing detection methods, at least in part, but also suggests the existence of a more complicated mechanism underlying the variable response to 5-ALA in tumor.

We also found that *ABCG2* and *PEPT1* showed altered expression levels associated with a modification of *CDH13* expression. *ABCG2* is well known as an ATP-binding efflux pump of porphyrin, indicating that the pump may be involved in the fluorescence induction mechanism of 5-ALA through the regulation of porphyrin transport.[1,35] In fact, inhibition of the *ABCG2* transporter has been shown to improve the efficacy of photodynamic therapy in keratinocytes.[3] Thus, our hypothesis is that *CDH13* downregulation may act on *ABCG2* to reduce the expression level and inhibit the efflux of PpIX and increase the accumulation of PpIX in glioma. We also revealed that *PEPT1* was upregulated in response to the *CDH13* downregulation in U251 cells. *PEPT1* is a 5-ALA influx transporter that may enhance PpIX accumulation,[19] although the expression level of *PEPT1* in control cells was extremely low and thus the increased effect was not definitive in this study. Some reports have found that *CDH13* possibly interacts with a transmembrane receptor, such as receptor tyrosine kinases or G protein-coupled receptors, to send a signal to Akt.[2] Given all of these data, *CDH13* might determine the intensity of the tumor fluorescence signal induced by 5-ALA by regulating PpIX accumulation into cells with modification of *ABCG2* and *PEPT1* expression via these signaling cascades. At present, the precise mechanisms remain unclear. We continue to intensely study the interaction of *CDH13* on *ABCB2* and *PEPT1* and the mechanistic roles in PpIX accumulation, along with a validation study of the correlation between CDH13 expression level and 5-ALA–induced fluorescence using more tumor specimens that showed different levels of fluorescence.

Conclusions

Our study demonstrated that *CDH13* might be the noteworthy factor in the mechanism of the 5-ALA–induced fluorescence signal, and its knockdown could enhance the intensity of the 5-ALA–induced fluorescence signal through an increase of PpIX accumulation in glioma cells. These new findings might lead a novel fluorescent indicator to overcome the obstacles of existing fluorescence-guided resection and improve the limited resection rate. Nevertheless, the details of *CDH13* actions in the 5-ALA metabolic pathway, including the interaction with *ABCB2* and *PEPT1*, remain unknown. Other than our suggested factors, there are several possible factors that might be involved in porphyrin biosynthesis, such as *FECH* and *CPOX*, but their functional significances remain controversial.[12] Further studies to clarify the roles of *CDH13* in the 5-ALA metabolic pathway are strongly required, along with studies involving the clinical application of these findings.

Acknowledgments

We thank Mss. Hitomi Miyabara, Azusa Sekine, Chieko Yanagidate, Chika Kumazawa, and Kyoko Totake for their enormous efforts and skillful technical assistance.

Disclosure

This study was performed as a research program of the Project for Development of Innovative Research on Cancer Therapeutics (P-Direct) from the Ministry of Education, Culture, Sport, Science, and Technology, Japan (MEXT). Additional support was provided by the National Cancer Center Research and Development Fund

(grant no. 23-A-20), the Strategic Research Foundation Grant-aided Project for Private Universities, MEXT (grant no. S0801004), and a Saitama Medical University Internal Grant (no. 08-1-1-11).

Author contributions to the study and manuscript preparation include the following. Conception and design: Nishiyama, Suzuki, Wada, Matsutani, Nishikawa. Acquisition of data: Suzuki, Wada, Eguchi, Adachi, Mishima, Nishikawa. Analysis and interpretation of data: Nishiyama, Suzuki, Wada, Eguchi, Adachi. Drafting the article: Nishiyama, Suzuki, Wada. Critically revising the article: all authors. Reviewed submitted version of manuscript: all authors. Approved the final version of the manuscript on behalf of all authors: Nishiyama. Statistical analysis: Wada, Eguchi. Administrative/technical/material support: Mishima, Matsutani, Nishikawa. Study supervision: Nishiyama, Nishikawa.

References

1. An R, Hagiya Y, Tamura A, Li S, Saito H, Tokushima D, et al: Cellular phototoxicity evoked through the inhibition of human ABC transporter ABCG2 by cyclin-dependent kinase inhibitors in vitro. **Pharm Res 26:**449–458, 2009
2. Andreeva AV, Kutuzov MA: Cadherin 13 in cancer. **Genes Chromosomes Cancer 49:**775–790, 2010
3. Bebes A, Nagy T, Bata-Csörgo Z, Kemény L, Dobozy A, Széll M: Specific inhibition of the ABCG2 transporter could improve the efficacy of photodynamic therapy. **J Photochem Photobiol B 105:**162–166, 2011
4. Bisland SK, Goebel EA, Hassanali NS, Johnson C, Wilson BC: Increased expression of mitochondrial benzodiazepine receptors following low-level light treatment facilitates enhanced protoporphyrin IX production in glioma-derived cells in vitro. **Lasers Surg Med 39:**678–684, 2007
5. Gupta N, Martin PM, Miyauchi S, Ananth S, Herdman AV, Martindale RG, et al: Down-regulation of BCRP/ABCG2 in colorectal and cervical cancer. **Biochem Biophys Res Commun 343:**571–577, 2006
6. Hefti M, von Campe G, Moschopulos M, Siegner A, Looser H, Landolt H: 5-aminolevulinic acid induced protoporphyrin IX fluorescence in high-grade glioma surgery: a one-year experience at a single institutuion. **Swiss Med Wkly 138:**180–185, 2008
7. Hinnen P, de Rooij FW, van Velthuysen ML, Edixhoven A, van Hillegersberg R, Tilanus HW, et al: Biochemical basis of 5-aminolaevulinic acid-induced protoporphyrin IX accumulation: a study in patients with (pre)malignant lesions of the oesophagus. **Br J Cancer 78:**679–682, 1998
8. Huang ZY, Wu Y, Hedrick N, Gutmann DH: T-cadherin-mediated cell growth regulation involves G2 phase arrest and requires p21(CIP1/WAF1) expression. **Mol Cell Biol 23:**566–578, 2003
9. Iacob G, Dinca EB: Current data and strategy in glioblastoma multiforme. **J Med Life 2:**386–393, 2009
10. Inoue H, Kajimoto Y, Shibata MA, Miyoshi N, Ogawa N, Miyatake S, et al: Massive apoptotic cell death of human glioma cells via a mitochondrial pathway following 5-aminolevulinic acid-mediated photodynamic therapy. **J Neurooncol 83:**223–231, 2007
11. Ishikawa T, Nakagawa H, Hagiya Y, Nonoguchi N, Miyatake S, Kuroiwa T: Key role of human ABC transporter ABCG2 in photodynamic therapy and photodynamic diagnosis. **Adv Pharmacol Sci 2010:**587306, 2010
12. Krishnamurthy P, Xie T, Schuetz JD: The role of transporters in cellular heme and porphyrin homeostasis. **Pharmacol Ther 114:**345–358, 2007
13. Lacroix M, Abi-Said D, Fourney DR, Gokaslan ZL, Shi W, DeMonte F, et al: A multivariate analysis of 416 patients with glioblastoma multiforme: prognosis, extent of resection, and survival. **J Neurosurg 95:**190–198, 2001
14. Lefranc F, Sadeghi N, Camby I, Metens T, Dewitte O, Kiss R: Present and potential future issues in glioblastoma treatment. **Expert Rev Anticancer Ther 6:**719–732, 2006
15. Li F, Glinskii OV, Zhou J, Wilson LS, Barnes S, Anthony DC, et al: Identification and analysis of signaling networks potentially involved in breast carcinoma metastasis to the brain. **PLoS ONE 6:**e21977, 2011
16. Miyake M, Ishii M, Kawashima K, Kodama T, Sugano K, Fujimoto K, et al: siRNA-mediated knockdown of the heme synthesis and degradation pathways: modulation of treatment effect of 5-aminolevulinic acid-based photodynamic therapy in urothelial cancer cell lines. **Photochem Photobiol 85:**1020–1027, 2009
17. Mohammed Ael S, Eguchi H, Wada S, Koyama N, Shimizu M, Otani K, et al: TMEM158 and FBLP1 as novel marker genes of cisplatin sensitivity in non-small cell lung cancer cells. **Exp Lung Res 38:**463–474, 2012
18. Nabavi A, Thurm H, Zountsas B, Pietsch T, Lanfermann H, Pichlmeier U, et al: Five-aminolevulinic acid for fluorescence-guided resection of recurrent malignant gliomas: a phase II study. **Neurosurgery 65:**1070–1077, 2009
19. Neumann J, Brandsch M: Delta-aminolevulinic acid transport in cancer cells of the human extrahepatic biliary duct. **J Pharmacol Exp Ther 305:**219–224, 2003
20. Ruge JR, Liu J: Use of 5-aminolevulinic acid for visualization and resection of a benign pediatric brain tumor. Case report. **J Neurosurg Pediatr 4:**484–486, 2009
21. Sanai N, Snyder LA, Honea NJ, Coons SW, Eschbacher JM, Smith KA, et al: Intraoperative confocal microscopy in the visualization of 5-aminolevulinic acid fluorescence in low-grade gliomas. Clinical article. **J Neurosurg 115:**740–748, 2011
22. Sano H, Wada S, Eguchi H, Osaki A, Saeki T, Nishiyama M: Quantitative prediction of tumor response to neoadjuvant chemotherapy in breast cancer: novel marker genes and prediction model using the expression levels. **Breast Cancer 19:**37–45, 2012
23. Sinha AK, Anand S, Ortel BJ, Chang Y, Mai Z, Hasan T, et al: Methotrexate used in combination with aminolaevulinic acid for photodynamic killing of prostate cancer cells. **Br J Cancer 95:**485–495, 2006
24. Smith JS, Chang EF, Lamborn KR, Chang SM, Prados MD, Cha S, et al: Role of extent of resection in the long-term outcome of low-grade hemispheric gliomas. **J Clin Oncol 26:** 1338–1345, 2008
25. Stepp H, Beck T, Pongratz T, Meinel T, Kreth FW, Tonn JCh, et al: ALA and malignant glioma: fluorescence-guided resection and photodynamic treatment. **J Environ Pathol Toxicol Oncol 26:**157–164, 2007
26. Stummer W, Novotny A, Stepp H, Goetz C, Bise K, Reulen HJ: Fluorescence-guided resection of glioblastoma multiforme by using 5-aminolevulinic acid-induced porphyrins: a prospective study in 52 consecutive patients. **J Neurosurg 93:** 1003–1013, 2000
27. Stummer W, Pichlmeier U, Meinel T, Wiestler OD, Zanella F, Reulen HJ: Fluorescence-guided surgery with 5-aminolevulinic acid for resection of malignant glioma: a randomised controlled multicentre phase III trial. **Lancet Oncol 7:**392–401, 2006
28. Stummer W, Stocker S, Wagner S, Stepp H, Fritsch C, Goetz C, et al: Intraoperative detection of malignant gliomas by 5-aminolevulinic acid-induced porphyrin fluorescence. **Neurosurgery 42:**518–526, 1998
29. Stupp R, Mason WP, van den Bent MJ, Weller M, Fisher B, Taphoorn MJ, et al: Radiotherapy plus concomitant and adjuvant temozolomide for glioblastoma. **N Engl J Med 352:**987–996, 2005
30. Takahashi K, Ikeda N, Nonoguchi N, Kajimoto Y, Miyatake S, Hagiya Y, et al: Enhanced expression of coproporphyrinogen oxidase in malignant brain tumors: CPOX expression and

5-ALA-induced fluorescence. **Neuro Oncol 13:**1234–1243, 2011
31. Takeuchi T, Misaki A, Liang SB, Tachibana A, Hayashi N, Sonobe H, et al: Expression of T-cadherin (CDH13, H-Cadherin) in human brain and its characteristics as a negative growth regulator of epidermal growth factor in neuroblastoma cells. **J Neurochem 74:**1489–1497, 2000
32. Teng L, Nakada M, Zhao SG, Endo Y, Furuyama N, Nambu E, et al: Silencing of ferrochelatase enhances 5-aminolevulinic acid-based fluorescence and photodynamic therapy efficacy. **Br J Cancer 104:**798–807, 2011
33. Tonn JC, Stummer W: Fluorescence-guided resection of malignant gliomas using 5-aminolevulinic acid: practical use, risks, and pitfalls. **Clin Neurosurg 55:**20–26, 2008
34. Tusher VG, Tibshirani R, Chu G: Significance analysis of microarrays applied to the ionizing radiation response. **Proc Natl Acad Sci U S A 98:**5116–5121, 2001
35. Wakabayashi K, Tamura A, Saito H, Onishi Y, Ishikawa T: Human ABC transporter ABCG2 in xenobiotic protection and redox biology. **Drug Metab Rev 38:**371–391, 2006

Manuscript submitted December 11, 2012.
Accepted July 22, 2013.
Please include this information when citing this paper: published online September 6, 2013; DOI: 10.3171/2013.7.JNS122340.
Address correspondence to: Masahiko Nishiyama, M.D., Ph.D., Department of Molecular Pharmacology and Oncology, Gunma University Graduate School of Medicine, 3-39-22 Showa-machi, Maebashi, Gunma 371-8511, Japan. email: m.nishiyama@gunma-u.ac.jp.

J Neurosurg 119:845–852, 2013

Phase II clinical study on intraoperative photodynamic therapy with talaporfin sodium and semiconductor laser in patients with malignant brain tumors

Clinical article

Yoshihiro Muragaki, M.D., Ph.D.,[1,2] Jiro Akimoto, M.D., D.Med.Sci.,[3] Takashi Maruyama, M.D., Ph.D.,[1,2] Hiroshi Iseki, M.D., Ph.D.,[1,2] Soko Ikuta, Ph.D.,[1] Masayuki Nitta, M.D., Ph.D.,[1,2] Katsuya Maebayashi, M.D., Ph.D.,[4] Taiichi Saito, M.D., Ph.D.,[1,5] Yoshikazu Okada, M.D., Ph.D.,[2] Sadao Kaneko, M.D.,[6] Akira Matsumura, M.D., Ph.D.,[7] Toshihiko Kuroiwa, M.D., Ph.D.,[8] Katsuyuki Karasawa, M.D., Ph.D.,[9] Yoichi Nakazato, M.D., Ph.D.,[10] and Takamasa Kayama, M.D., Ph.D.[11]

[1]Faculty of Advanced Techno-Surgery, Institute of Advanced Biomedical Engineering and Science, and Departments of [2]Neurosurgery and [4]Radiation Oncology, Tokyo Women's Medical University, Tokyo; [3]Department of Neurosurgery, Tokyo Medical University, Tokyo; [5]Department of Neurosurgery, Hiroshima University, Hiroshima; [6]Kashiwaba Neurosurgical Hospital, Sapporo; [7]Department of Neurosurgery, University of Tsukuba, Ibaragi; [8]Department of Neurosurgery, Osaka Medical College, Osaka; [9]Department of Radiology, Tokyo Metropolitan Cancer and Infectious Diseases Center, Komagome Hospital, Tokyo; [10]Department of Human Pathology, Gunma University Graduate School of Medicine, Gunma; and [11]Department of Neurosurgery, Yamagata University, Yamagata, Japan

Object. The objective of the present study was to perform a prospective evaluation of the potential efficacy and safety of intraoperative photodynamic therapy (PDT) using talaporfin sodium and irradiation using a 664-nm semiconductor laser in patients with primary malignant parenchymal brain tumors.

Methods. In 27 patients with suspected newly diagnosed or recurrent primary malignant parenchymal brain tumors, a single intravenous injection of talaporfin sodium (40 mg/m^2) was administered 1 day before resection of the neoplasm. The next day after completion of the tumor removal, the residual lesion and/or resection cavity were irradiated using a 664-nm semiconductor laser with a radiation power density of 150 mW/cm^2 and a radiation energy density of 27 J/cm^2. The procedure was performed 22–27 hours after drug administration. The study cohort included 22 patients with a histopathologically confirmed diagnosis of primary malignant parenchymal brain tumor. Thirteen of these neoplasms (59.1%) were newly diagnosed glioblastomas multiforme (GBM).

Results. Among all 22 patients included in the study cohort, the 12-month overall survival (OS), 6-month progression-free survival (PFS), and 6-month local PFS rates after surgery and PDT were 95.5%, 91%, and 91%, respectively. Among patients with newly diagnosed GBMs, all these parameters were 100%. Side effects on the skin, which could be attributable to the administration of talaporfin sodium, were noted in 7.4% of patients and included rash (2 cases), blister (1 case), and erythema (1 case). Skin photosensitivity test results were relatively mild and fully disappeared within 15 days after administration of photosensitizer in all patients.

Conclusions. Intraoperative PDT using talaporfin sodium and a semiconductor laser may be considered as a potentially effective and sufficiently safe option for adjuvant management of primary malignant parenchymal brain tumors. The inclusion of intraoperative PDT in a combined treatment strategy may have a positive impact on OS and local tumor control, particularly in patients with newly diagnosed GBMs. Clinical trial registration no.: JMA-IIA00026 (https://dbcentre3.jmacct.med.or.jp/jmactr/App/JMACTRS06/JMACTRS06.aspx?seqno=862).
(http://thejns.org/doi/abs/10.3171/2013.7.JNS13415)

Key Words • **malignant brain tumor** • **malignant glioma** • **oncology** • **photodynamic therapy** • **talaporfin sodium** • **outcome**

Malignant brain tumors are characterized by invasive growth into adjacent normal neuronal tissue. Therefore, it is crucial that their man-

This article contains some figures that are displayed in color online but in black-and-white in the print edition.

Abbreviations used in this paper: GBM = glioblastoma multiforme; OS = overall survival; PDT = photodynamic therapy; PFS = progression-free survival; PS = performance status; 5-ALA = 5-aminolevulinic acid.

agement is directed not only to maximal possible resection (while ensuring preservation of the functionally important anatomical structures), but on suppressing the growth of the residual infiltrative tumor cells. Despite aggressive surgical removal followed by postoperative radiotherapy and chemotherapy, between 50% and 85% of WHO Grade IV gliomas recur locally.[9,16] This emphasizes the need for additional options to improve their growth control.

Photodynamic therapy (PDT) is a treatment method that involves administration of a photosensitizer that accumulates in tumor tissue and newly formed neoplastic vessels. During subsequent irradiation with a laser beam of a specific wavelength, the photosensitizer undergoes a photochemical reaction that produces singlet oxygen possessing strong oxidation properties that cause alteration of the cells. Because singlet oxygen has a short lifetime (0.04–4 μsec), the PDT-induced cell death is realized only locally in the areas irradiated by the laser beam.[2,7,8,15]

Talaporfin sodium (mono-L-aspartyl chlorine e6, or NPe6) is a relatively novel photosensitizer for PDT. Its administration in combination with a semiconductor laser has been approved in Japan for clinical use in cases of early stage lung cancer. Nonclinical pharmacological studies directed to its possible application for management of malignant brain tumors were initiated starting in 2001.[12–14] Experiments with glioblastoma cell lines demonstrated that such therapy induces mitochondrial apoptotic cell loss accompanied by tumor necrosis.[13,14] Our recent single-center pilot clinical study on the use of talaporfin sodium and a semiconductor laser in patients with malignant gliomas demonstrated promising results with regard to tumor response rates and treatment safety.[1] Therefore, the present open-label, prospective, multicenter clinical trial was initiated for evaluation of the potential efficacy and safety of such therapy. This study was the first investigator-initiated clinical trial in Japan that planned to assess the use of talaporfin sodium and a semiconductor laser for intraoperative PDT as part of a combined management of primary malignant parenchymal brain tumors.

Methods

Patients with suspected primary malignant parenchymal brain tumors, either newly diagnosed or recurrent, which according to preoperative neuroimaging corresponded to a WHO histopathological grade of III or IV,[11] were enrolled in this study. The recruitment of patients and analysis of treatment efficacy were mainly focused on newly diagnosed glioblastoma multiforme (GBM). The main inclusion criteria included agreement of the patient to provide written informed consent to participate in the study; age between 20 and 69 years at the time of informed consent; performance status (PS) score of 0, 1, 2, or 3 according to Eastern Cooperative Oncology Group PS scale (a PS score of 3 was accepted only when the score was attributable to neurological symptoms caused by the tumor); supratentorial location of the tumor not including neoplasms originating from the optic pathways and pituitary gland; absence of subarachnoid dissemination; and eligibility for aggressive resection of the lesion. The main exclusion criterion was a history of photosensitivity or porphyria.

Study Design

This prospective clinical trial was developed and carried out in 2 neurosurgical centers with well-established neurooncology programs, namely Tokyo Women's Medical University and Tokyo Medical University. An open-label, investigator-initiated clinical study was conducted in accordance with the Declaration of Helsinki. The research protocol was approved by the Pharmaceuticals and Medical Devices Agency of Japan as well as by the ethics committees and institutional review boards of both participating universities. A special review board was formed for central radiology assessment, evaluation of data related to treatment efficacy and safety, and handling of the enrolled cases and overall data management. Additionally, a pathology board was created for central review of the permanent formalin-fixed tissue specimens to determine the histopathological tumor type and grade. The 3-year study period was scheduled from March 21, 2009, to February 28, 2012. The clinical trial information for this study can be found at https://dbcentre3.jmacct.med.or.jp/jmactr/App/JMACTRS06/JMACTRS06.aspx?seqno=862.

Patients who were considered eligible for enrollment into study received a single intravenous injection of talaporfin sodium (Laserphyrin, Meiji Seika Pharma Co., Ltd.) in a dose of 40 mg/m^2 on an inpatient basis 1 day prior to undergoing the elective craniotomy. The next day, surgery was done, the neoplasm was resected, and irradiation of the resection cavity with a 664-nm semiconductor laser beam (Panasonic Healthcare Co., Ltd.), with a diameter of 1.5 cm, radiation power density of 150 mW/cm^2, and radiation energy density of 27 J/cm^2, was performed. Particular emphasis was put on irradiation of the areas at risk for recurrence, such as the genu of the corpus callosum.[9] If tumor resection was incomplete and the residual lesion was macroscopically identified, additional irradiation by the laser was applied at 1 to 3 sites with avoidance of overlap of the irradiation areas. In all cases laser irradiation was done 22–27 hours after administration of talaporfin sodium.

Postoperative Treatment and Follow-Up

Postoperatively all patients with newly diagnosed gliomas underwent fractionated radiotherapy (total dose 60 Gy) with concomitant and adjuvant chemotherapy using ACNU (in cases of WHO Grade III tumors) or temozolomide[18] (in cases of GBM). Patients with recurrent neoplasms were treated according to the preference of their doctors, taking into consideration the details of the primary management.

Adverse effects of treatment were graded according to the Common Terminology Criteria for Adverse Events version 3.0.[3] Follow-up examinations were performed every 2–3 months and included physical and neurological assessments with evaluation of PS score, blood and urine tests, and contrast-enhanced MRI. Tumor progression was defined as a 25% or greater increase in the volume of the contrast-enhanced lesion or the appearance of

new brain lesions. At the time of recurrence the salvage treatment was applied according to the preference of the individual doctors and usually included a combination of re-resection, second-line chemotherapy, and/or vaccine therapy.

End Point Evaluation

The primary end point of the study was overall survival (OS) rate at 12 months after PDT. Secondary end points were progression-free survival (PFS) and local PFS rates at 6 months after PDT. The OS, PFS, and local PFS were all estimated from the date of surgery. Additionally, in cases with a maximal diameter of the residual neoplasm of 16 mm or more, the overall tumor response to treatment was evaluated. All brain MRI data before surgery and during follow-up were assessed by review board members. Safety end points included rates of adverse events, side effects, and results of skin photosensitivity testing.

Data Analysis

Analysis of the treatment efficacy was done in all patients who underwent PDT based on administration of talaporfin sodium and intraoperative laser irradiation of the residual neoplasm and/or resection cavity if the diagnosis of primary malignant parenchymal brain tumor was confirmed by the pathology review board after investigation of the permanent formalin-fixed tissue sections (study cohort). Separate analysis of the treatment efficacy was also done in the subgroup of patients with newly diagnosed GBMs. Survival was assessed using the Kaplan-Meier method. Analysis of the treatment safety was done in all patients initially enrolled into the study who received talaporfin sodium.

Results

Patient Characteristics

Detailed characteristics of patients enrolled in the study are presented in Table 1. In all, 27 patients initially received talaporfin sodium. However, 3 patients were deemed ineligible for study participation during surgery and did not receive irradiation with the laser based on the results of the intraoperative histopathological investigation of the resected tissue on the frozen sections, which revealed lymphoma, low-grade glioma, and cavernoma (1 case each). Additionally, 2 patients were excluded from the study later on because the pathology review board did not confirm the diagnosis of a primary malignant parenchymal brain tumor based on the postoperative examination of the permanent formalin-fixed tissue sections. Therefore, the study cohort included 22 patients with a male/female ratio of 1:1 and a median age of 50.5 years (range 24–69 years). The frontal lobe was affected most frequently (59.1% of cases). In 72.7% of patients the tumor was located within or close to eloquent brain areas. Total, subtotal (> 90% of the lesion volume), and partial resections of the neoplasm were performed in 36.4%, 50%, and 13.6% of cases, respectively. No significant differences in clinical characteristics were observed between the entire group of initially enrolled patients (n = 27) and the study cohort (n = 22). Thirteen (59.1%) of 22 patients included in the study cohort had newly diagnosed GBMs and corresponded to recursive partitioning analysis Classes III (4 cases), IV (5 cases), and V (4 cases).[6]

Treatment Efficacy

Among all 22 patients included in the study cohort, 1 death occurred within 12 months after surgery. This patient died 3.4 months after resection and PDT of a newly diagnosed gliosarcoma due to local progression of the tumor. Therefore, the 12-month OS rate was 95.5%. Two tumors demonstrated progression despite treatment within 6 months after surgery, and both recurrences were local. Therefore, the 6-month PFS and local PFS rates were 91%. The maximum length of follow-up was 38.6 months. The median OS was 27.9 months (95% CI lower, 24.8 months; upper, not estimated), the median PFS was 20 months (95% CI lower, 10.3 months; upper, not estimated), and the median local PFS was 22.5 months (95% CI lower, 17.2 months; upper, not estimated).

Among 13 patients with newly diagnosed GBM, the 12-month OS, 6-month PFS, and 6-month local PFS rates after surgical removal of the tumor and PDT were all 100% (Fig. 1). In this subgroup the maximum length of follow-up was 32.0 months. The median OS was 24.8 months (95% CI 18.5–32.0 months), the median PFS was 12.0 months (95% CI 10.3–24.2 months), and the median local PFS was 20.0 months (95% CI 16.2–32.0 months).

In only 1 patient was it possible to evaluate the overall tumor response to treatment. In this case, a newly diagnosed GBM showed complete response 4 months after surgery and PDT.

Treatment Safety

Among all 27 patients who received talaporfin sodium the day before surgery, serious adverse events were noted postoperatively in 6 patients (22.2%). These included aphasia (2 cases) and hemiplegia, hemiparesis, unilateral blindness, visual field defect, homonymous hemianopia, postoperative pyrexia, and infection (1 case each). The overall frequency and distribution of postoperative adverse events were within the range of our usual neurosurgical practice in cases of primary malignant parenchymal brain tumors, and their causal relationships with administration of talaporfin sodium and/or intraoperative laser irradiation were very unlikely. None of these adverse events resulted in the death of a patient.

The laboratory test results in all patients were abnormal, most frequently with an increase in γ-glutamyltransferase (59.3%), alanine aminotransferase (48.1%), aspartate aminotransferase (37.0%), blood alkaline phosphatase (25.9%), and blood lactate dehydrogenase (22.2%). In 18 (66.7%) of 27 patients such abnormalities could be considered as side effects after administration of talaporfin sodium. Postoperative adverse events by system organs, particularly abnormal liver function, were relatively frequent but never exceeded Grade 3 toxicity (Table 2). Only 2 patients (7.4%) had skin disorders, which could be con-